Human mitochondrial cytochrome P450 27C1 is localized in skin and preferentially desaturates *trans*-retinol to 3,4-dehydroretinol

Received for publication, December 22, 2016, and in revised form, June 29, 2017 Published, Papers in Press, July 12, 2017, DOI 10.1074/jbc.M116.773937

Kevin M. Johnson, Thanh T. N. Phan, Matthew E. Albertolle, and F. Peter Guengerich[1]

From the Department of Biochemistry, Vanderbilt University School of Medicine, Nashville, Tennessee 37232-0146

Edited by Ruma Banerjee

Recently, zebrafish and human cytochrome P450 (P450) 27C1 enzymes have been shown to be retinoid 3,4-desaturases. The enzyme is unusual among mammalian P450s in that the predominant oxidation is a desaturation and in that hydroxylation represents only a minor pathway. We show by proteomic analysis that P450 27C1 is localized to human skin, with two proteins of different sizes present, one being a cleavage product of the full-length form. P450 27C1 oxidized all-*trans*-retinol to 3,4-dehydroretinol, 4-hydroxy (OH) retinol, and 3-OH retinol in a 100:3:2 ratio. Neither 3-OH nor 4-OH retinol was an intermediate in desaturation. No kinetic burst was observed in the steady state; neither the rate of substrate binding nor product release was rate-limiting. Ferric P450 27C1 reduction by adrenodoxin was 3-fold faster in the presence of the substrate and was ~5-fold faster than the overall turnover. Kinetic isotope effects of 1.5–2.3 (on k_{cat}/K_m) were observed with 3,3-, 4,4-, and 3,3,4,4-deuterated retinol. Deuteration at C-4 produced a 4-fold increase in 3-hydroxylation due to metabolic switching, with no observable effect on 4-hydroxylation. Deuteration at C-3 produced a strong kinetic isotope effect for 3-hydroxylation but not 4-hydroxylation. Analysis of the products of deuterated retinol showed a lack of scrambling of a putative allylic radical at C-3 and C-4. We conclude that the most likely catalytic mechanism begins with abstraction of a hydrogen atom from C-4 (or possibly C-3) initiating the desaturation pathway, followed by a sequential abstraction of a hydrogen atom or proton-coupled electron transfer. Adrenodoxin reduction and hydrogen abstraction both contribute to rate limitation.

Cytochrome P450 (P450)[2] enzymes are rather ubiquitous in nature. The mammalian P450 enzymes are important in drug and carcinogen metabolism (2, 3) and also have critical roles in steroid metabolism (4). In addition, P450s have important roles in the metabolism of vitamins A, D, E, and K (5).

Of the 57 human P450 genes, 50 code for proteins that are localized mainly in the endoplasmic reticulum, and seven code for P450s that are nucleus-encoded and transported to mitochondria (5). These seven P450s utilize adrenodoxin (Adx), a ferredoxin, as a source of electrons, instead of the flavoprotein NADPH-P450 reductase used by the P450s in the endoplasmic reticulum (Fig. 1). In addition, a complement of some of the microsomal P450s is also found in mitochondria, and these P450s also utilize electrons from Adx (6, 7). Of the seven mammalian mitochondrial P450s, X-ray crystal structures of three have been reported (11A1, 11B2, and 24A1) (8–11). Only P450s 11A1 and 11B1 have been extensively characterized in terms of their interactions with Adx and their catalytic mechanisms (12–21).

Substrates remain unknown for some of the P450s, including human P450s (22). In 2006, our laboratory expressed and characterized one of these "orphan" P450s, P450 27C1 (23). However, no substrates could be identified at that time. Subsequently, both zebrafish (24) and human (25) P450 27C1 were found to catalyze the 3,4-desaturation of retinoids, particularly all-*trans*-retinol (Fig. 2). The human enzyme also formed a minor product that co-migrated (HPLC) with 4-hydroxyretinol (25).

Desaturation reactions are common in fatty acid metabolism. However, the enzymes that catalyze these reactions are generally non-heme iron monooxygenases (26, 27). Some yeast and bacterial P450s are desaturases (*e.g.* P450s 61 and 710A) (28–31). However, with mammalian P450s, desaturation reactions occasionally accompany hydroxylations but represent only minor pathways (32–36). The reasons for the balance between hydroxylation and desaturation have been considered at a theoretical level (27, 37, 38), and it has been possible to modulate the ratio of these reactions catalyzed by a bacterial P450 through site-directed mutagenesis (39, 40).

In this work, we established the localization of human P450 27C1 in skin. Both 3- and 4-hydroxyretinol were characterized as minor products of P450 27C1. Kinetic isotope effect (KIE) studies with 3- and 4-deuterated retinol showed contributions of C–H bond breaking as a rate-limiting step in catalysis of

This work was supported, in whole or in part, by National Institutes of Health Grants R01 GM118122 (to F. P. G.), T32 CA009582 (to K. M. J.), and T32 ES007028 (to M. E. A.) and American Heart Association Predoctoral Fellowship PRE33410007 (to M. E. A.). The authors declare that they have no conflicts of interest with the contents of this article. The content is solely the responsibility of the authors and does not necessarily represent the official views of the National Institutes of Health.

This article contains supplemental Table S1 and Figs. S1–S8.

[1] To whom correspondence should be addressed: Dept. of Biochemistry, Vanderbilt University School of Medicine, 638B Robinson Research Bldg., 2200 Pierce Ave., Nashville, TN 37232-0146. Tel.: 615-322-2261; Fax: 615-343-0704; E-mail: f.guengerich@vanderbilt.edu.

[2] The abbreviations used are: P450, cytochrome P450; ADR, NADPH-adrenodoxin reductase; Adx, adrenodoxin; APCI, atmospheric pressure chemical ionization; HRMS, high-resolution mass spectrometry; KIE, kinetic (deuterium) isotope effect; HCD, higher-energy collisional dissociation; AGC, automatic gain control; SVD, single-variable decomposition.

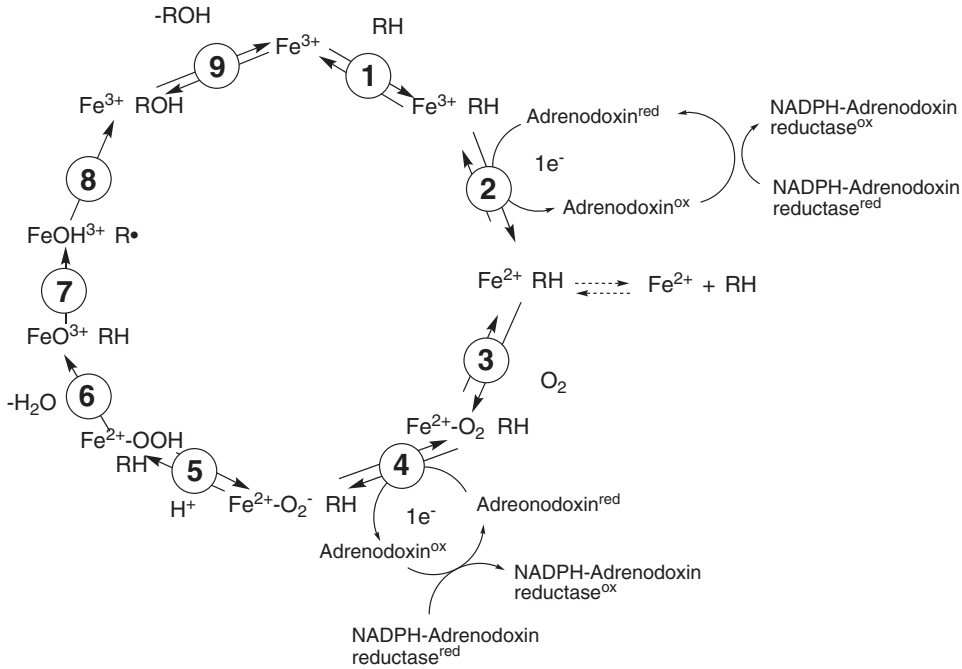

Figure 1. General catalytic cycle for mitochondrial P450s. Steps are indicated with numbers.

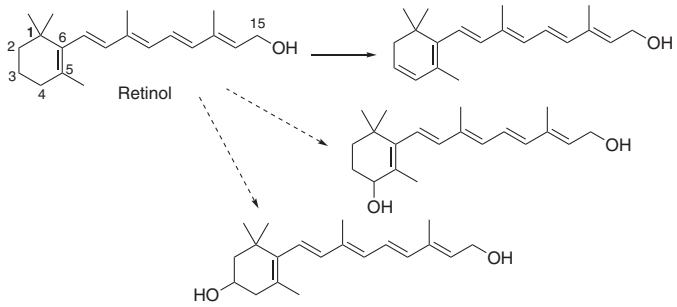

Figure 2. Oxidation of all-*trans*-retinol by P450 27C1. Relevant carbon atoms are indicated with numbers.

desaturation and the hydroxylations. Kinetic analysis of other steps in the reaction cycle indicated that P450 27C1 reduction by Adx also contributes in terms of rate limitation.

Results

Identification of P450 27C1 in skin by mass spectrometry and immunochemical methods

MS profiling was done with human liver and skin samples, based on previous work showing P450 27C1 mRNA in the liver (23) and the demonstration of retinol desaturation activity in human skin epidermis (41). Because P450 27C1 is considered to be a mitochondrial protein (due to sequence similarity to P450s 27A1 and 27B1 and the demonstrated reduction by Adx (24)), we utilized tissue homogenates instead of microsomal fractions. Human P450 27C1 is 43% identical to P450 27A1 (a liver enzyme (5)) and 38% identical to P450 27B1 (a kidney enzyme (5)), based on Uniprot.org alignment (http://www.uniprot.org/align).[3] Purified recombinant P450 27C1 (see supplemental Fig. S1) was used to guide the selection of migration distances selected for analysis (the M_r is less because 66 residues were deleted from the N terminus in the construct that we used (GenBank™ accession number AC027142; March 28, 2000) (and two new ones were added at the N terminus and His_6 at the C terminus) (23)). The P450 27C1 sequence listed in Uniprot Q4G0S4 (and also as NG007986, NM_001001165, and AC027142 elsewhere) begins with MRSVLRQ, is only 372 residues long, and is missing the N-terminal 106 residues of our expressed P450 27C1 (23), based on the original sequence of Nelson (http://drnelson.uthsc.edu/cytochromeP450.html)[3] (95), which denotes the shortened sequences in that website. Initial LC-MS/MS of tryptic peptides from a human skin sample showed the presence of P450 27C1, with 51% sequence coverage in this 372-residue region (supplemental Table S1) (Fig. 3). We hypothesized that the 372-amino acid entry in the databases is an error due to misassignment of the methionine start site and did extensive proteomic analysis with a second skin sample (*i.e.* different individual) to define the protein found in human skin.

Polyclonal antibodies were raised against P450 27C1 and purified by adsorption with immobilized P450 27C1. Immunoblotting consistently showed the presence of two bands in all five human skin samples examined (Fig. 4*A*) but no detectable bands in any of the human liver or kidney samples, only background staining (Fig. 4, *B* and *C*) (the limit of detection was 0.1 pmol of P450 27C1). (Note that the tissue samples were not from the same five individuals.)

Because strong denaturing conditions were required to solubilize human skin samples, conventional methods for antibody pull-down experiments were not possible for validating the specificity of the antibody. Accordingly, we digested the proteins in the gel regions corresponding to antibody binding (Fig. 4). For the upper band, the estimated content varied from 11 to 14 pmol of P450 27C1 (mg of

[3] Please note that the JBC is not responsible for the long-term archiving and maintenance of this site or any other third party hosted site.

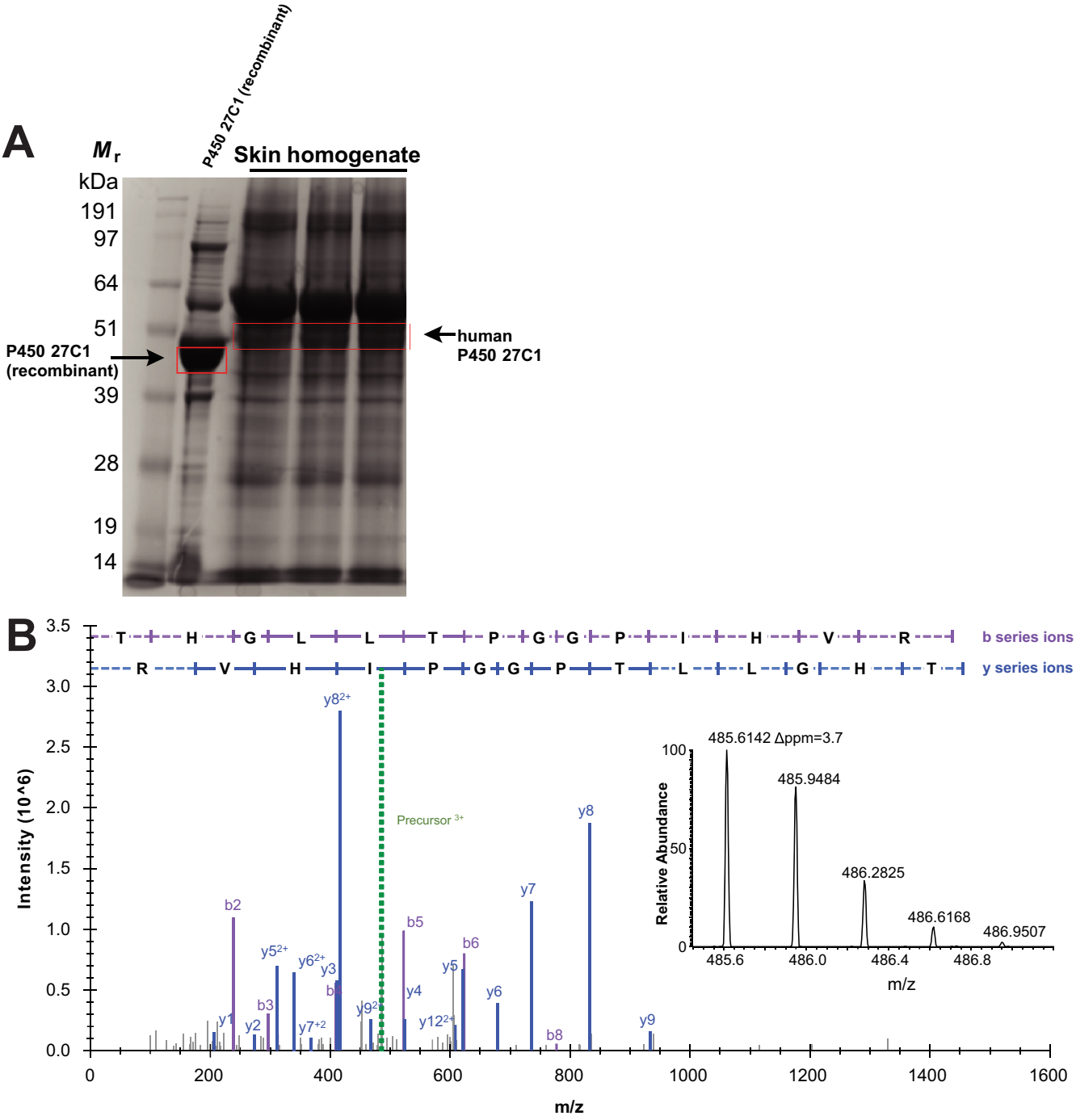

Figure 3. Proteomic analysis of human skin tissue homogenate. *A*, separation of human skin proteins by SDS-PAGE for in-gel trypsin digest of separated proteins (~130 μg of total protein/lane). Multiple gel sections were cut and analyzed by LC-MS/MS. *Boxes* drawn (*red*) show the gel slices excised containing either the recombinant P450 27C1 enzyme used as a standard or the identified human P450 27C1 present in the skin sample. (Note that the recombinant protein is 58 amino acids shorter than the native P450 27C1 (23).) *B*, representative LC-MS/MS fragmentation of peptide 354–367 (THGLLTPGGPIHVR), based on the numbering of the database 372 residue protein. The numbering for the fragment in the sequence presented in Fig. 5 is 524–537, and the same peptide is shown again in supplemental Fig. S3. Identified fragment ions are annotated and *color-coordinated* (*blue*, *y*-ions; *purple*, *b*-ions). *Heavy lines*, peptide fragments identified; *dashed lines*, missed fragment ions. Included is the precursor +3 ion (*inset*, isotopic distribution) identified and selected for fragmentation. The spectrum was generated using SeeMS for MS^2 data integrated into IDPicker software and Xcalibur Qual Browser for MS^1 data. See also supplemental Table S1.

protein)$^{-1}$ and from 5 to 11 pmol P450 27C1 (mg of protein)$^{-1}$ for the lower band.

Further proteomic analysis of the two gel regions was done. Peptides corresponding to both bands were identified, validating the specificity of our antibody (Fig. 5). The coverage was 37% in the upper band and ~40% in the lower one (depending on exactly where the N terminus is). The identification of the peptide MQTSAMALLAR (in the higher M_r band) (Fig. 5*A* and supplemental Fig. S2) indicates that this is the correct start site. We are not exactly sure what the N terminus of the lower band

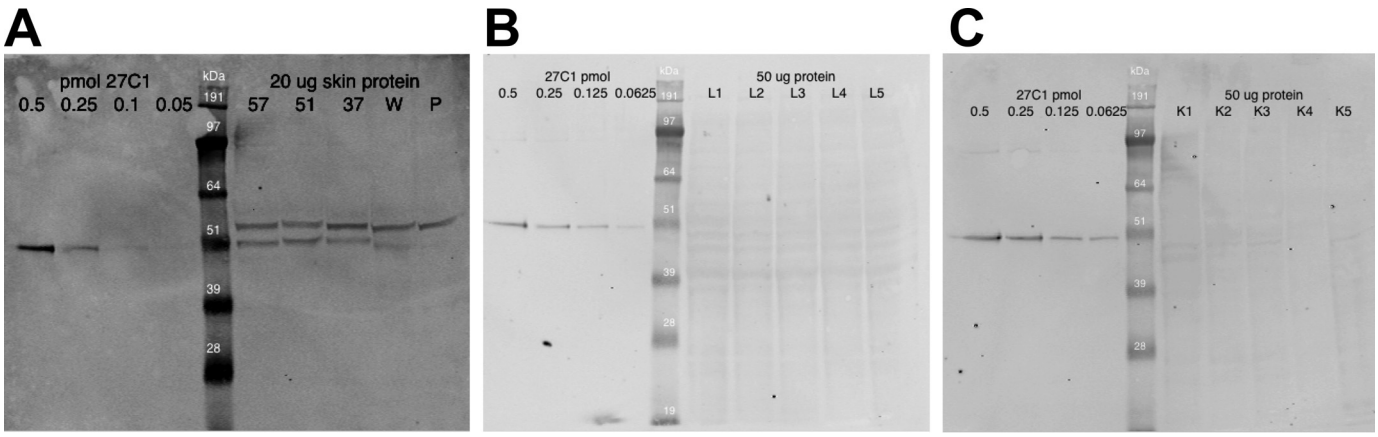

Figure 4. Immunoblot analysis of P450 27C1 in human skin, liver, and kidney homogenates. In each *panel*, each of the *left four lanes* of the gel included 0.5, 0.25, 0.10, and 0.05 pmol of purified P450 27C1. The six M_r markers are indicated in the *center lane*, along with M_r values (in kDa). The *five lanes* on the *right* in each *panel* include samples from five different humans (tissue homogenates). *A*, skin (nominal 20 μg of protein); *B*, liver (nominal 50 μg of protein); *C*, kidney (nominal 50 μg of protein). The samples in *A* were further normalized using staining of the transferred proteins with SyPro Ruby dye. The estimated contents of P450 27C1 in the five skin samples were as follows(*top band*/*bottom band*): *57*, 12/11 pmol/mg protein; *51*, 11/19 pmol/mg protein; *37*, 13/10 pmol/mg protein; *W*, 14/7 pmol/mg protein; *P*, 12/5 pmol/mg protein. Equal binding of antibody is assumed for the two bands, although we do not have specific evidence for this.

A

```
     1   5   10  15  20  25  30  35  40
 1   M Q T S A M A L L A R I L R A G L R P A P E R G G L L G G G A P R R P Q P A G A
41   R L P A G A R A E D K G A G R P G S P P G G G R A E G P R S L A A M P G P R T L
81   A N L A E F F C R D G F S R I H E I Q Q K H T R E Y G K I F K S H F G P Q F V V
121  S I A D R D M V A Q V L R A E G A A P Q R A N M E S W R E Y R D L R G R A T G L
161  I S A E G E Q W L K M R S V L R Q R I L K P K D V A I Y S G E V N Q V I A D L I
201  K R I Y L L R S Q A E D G E T V T N V N D L F F K Y S M E G V A T I L Y E S R L
241  G C L E N S I P Q L T V E Y I E A L E L M F S M F K T S M Y A G A I P R W L R P
281  F I P K P W R E F C R S W D G L F K F S Q I H V D N K L R D I Q Y Q M D R G R R
321  V S G G L L T Y L F L S Q A L T L Q E I Y A N V T E M L L A G V D T T S F T L S
361  W T V Y L L A R H P E V Q Q T V Y R E I V K N L G E R H V P T A A D V P K V P L
401  V R A L L K E T L R L F P V L P G N G R V T Q E D L V I G G Y L I P K G T Q L A
441  L C H Y A T S Y Q D E N F P R A K E F R P E R W L R K G D L D R V D N F G S I P
481  F G H G V R S C I G R R I A E L E I H L V V I Q L L Q H F E I K T S S Q T N A V
521  H A K T H G L L T P G G P I H V R F V N R K
```

B

```
     1   5   10  15  20  25  30  35  40
 1   M Q T S A M A L L A R I L R A G L R P A P E R G G L L G G G A P R R P Q P A G A
41   R L P A G A R A E D K G A G R P G S P P G G G R A E G P R S L A A M P G P R T L
81   A N L A E F F C R D G F S R I H E I Q Q K H T R E Y G K I F K S H F G P Q F V V
121  S I A D R D M V A Q V L R A E G A A P Q R A N M E S W R E Y R D L R G R A T G L
161  I S A E G E Q W L K M R S V L R Q R I L K P K D V A I Y S G E V N Q V I A D L I
201  K R I Y L L R S Q A E D G E T V T N V N D L F F K Y S M E G V A T I L Y E S R L
241  G C L E N S I P Q L T V E Y I E A L E L M F S M F K T S M Y A G A I P R W L R P
281  F I P K P W R E F C R S W D G L F K F S Q I H V D N K L R D I Q Y Q M D R G R R
321  V S G G L L T Y L F L S Q A L T L Q E I Y A N V T E M L L A G V D T T S F T L S
361  W T V Y L L A R H P E V Q Q T V Y R E I V K N L G E R H V P T A A D V P K V P L
401  V R A L L K E T L R L F P V L P G N G R V T Q E D L V I G G Y L I P K G T Q L A
441  L C H Y A T S Y Q D E N F P R A K E F R P E R W L R K G D L D R V D N F G S I P
481  F G H G V R S C I G R R I A E L E I H L V V I Q L L Q H F E I K T S S Q T N A V
521  H A K T H G L L T P G G P I H V R F V N R K
```

Figure 5. Proteomic analysis of a human skin sample and analysis of protein N terminus. Human skin sample 57 (Fig. 4) was used, and the two immunoreactive bands were located by comparison with a part of the same gel in which the proteins were transferred to a sheet of nitrocellulose and located by immunostaining (Fig. 4). *A*, predicted full-length amino acid sequence of P450 27C1, with *highlighted* and *underlined peptides* identified in the higher-M_r band of Fig. 4; see supplemental Figs. S2 and S3 for the N-terminal and most C-terminal peptides identified. *B*, predicted full-length amino acid sequence of P450 27C1, with *highlighted* and *underlined peptides* identified in the lower-M_r band of Fig. 4. See Fig. 3 and supplemental Table S1 for more data on peptide analysis with a sample from a different individual.

is. We did identify the peptide SLAAMPGPR (amino acids 70–78 in Fig. 5*B*) in an analysis. The C terminus is nearly intact, with the peptide THGLLTPGGPIHVR identified (in both bands; Fig. 5 and supplemental Fig. S3). Therefore the cleavage site is postulated to be near residue 70 (Fig. 5*C*), in that the M_r of the lower band is very similar to that of recombinant P450 27C1 (Fig. 4*A*), which is 58 residues shorter than the full-length sequence shown (23).

No P450 27C1 peptides were detected in a (single) human liver sample when a similar analysis was done under similar conditions (results not shown).

Identification of reaction products

Oxidation of all-trans-retinol to 3- and 4-OH products—We previously reported that human P450 27C1 oxidized retinol to a product that co-eluted with 4-OH retinol (Fig. 2), in addition to the desaturation product 3,4-dehydroretinol (25). However, we did not have any independent evidence for its identity. We synthesized both 3- and 4-OH retinol (supplemental Figs. S4 and S5) and found that both of these alcohols are minor products, based on co-chromatography by HPLC and UV and mass spectral comparisons. Because of the trace amounts of these products formed, we did not determine steady-state kinetic parameters for their production. At a substrate concentration of 7 μM, the molar ratio of products formed was 100:3:2 for 3,4-dehydroretinol, 4-OH retinol, and 3-retinol, respectively (Fig. 6). Incubation of 3- or 4-OH retinol with P450 27C1 (in the presence or absence of NADPH-Adx reductase (ADR), Adx, and NADPH) did not show any formation of 3,4-dehydroretinol, indicating that neither of the hydroxy compounds is an intermediate in the formation of dehydroretinol.

Other reactions—In previous studies, we found that retinoic acid and retinaldehyde (oxidized forms of all-*trans*-retinol) were substrates for P450 27C1, with lower catalytic activities compared with retinol (23, 24). We also tested two known biologically important retinyl esters as substrates with P450 27C1. Retinol acetate and retinol palmitate (20 μM) were incubated in the presence of P450 27C1, ADR, Adx, and NADPH. After mild KOH hydrolysis of reaction mixtures, 3,4-dehydroretinol was detected in the reaction with retinol acetate but not with retinol palmitate (data not shown).

Individual reaction steps and catalytic mechanism

Substrate binding—We had previously shown that human P450 27C1 forms a tight complex with all-*trans*-retinol, shifting the heme Soret peak from the low- to high-spin iron form ("Type I" difference spectrum), with an estimated K_d of ~5.6 nM (25). The rate of binding was measured using two different approaches. Equimolar concentrations of P450 27C1 and the substrate all-*trans*-retinol were mixed in a stopped-flow spectrophotometer (Fig. 7*A*), and the data (Fig. 7*B*) were fit to a second-order equation, in that the binding reaction is first-order in both P450 and substrate (42). The estimated k_{on} value was 1.9×10^5 M^{-1} s^{-1} (Fig. 7*C*). In an alternative approach, first-order rates were estimated with varying concentrations of substrate and plotted *versus* the substrate concentration (43) to obtain a k_{on} value of 1.6×10^5 M^{-1} s^{-1} and k_{off} of 0.022 s^{-1} (Fig. 7*D*). This k_{off} value is subject to considerable error because of the need to use ≥1 μM P450 in these stopped-flow measurements. A trapping assay was used in which a 1:1 molar mixture of 2 μM P450 27C1 and *trans*-retinol was mixed with 20 μM ketoconazole, an inhibitor that was measured to have a K_d of 7 ± 4 μM and gives a spectrally distinct complex with P450s ("Type II") (44). The observed rate was 0.017 s^{-1}, or 1 min^{-1} (compared with a rate of 1,200 ± 240 min^{-1} for ketoconazole binding to P450 27C1 in the absence of dehydroretinol; results not shown).

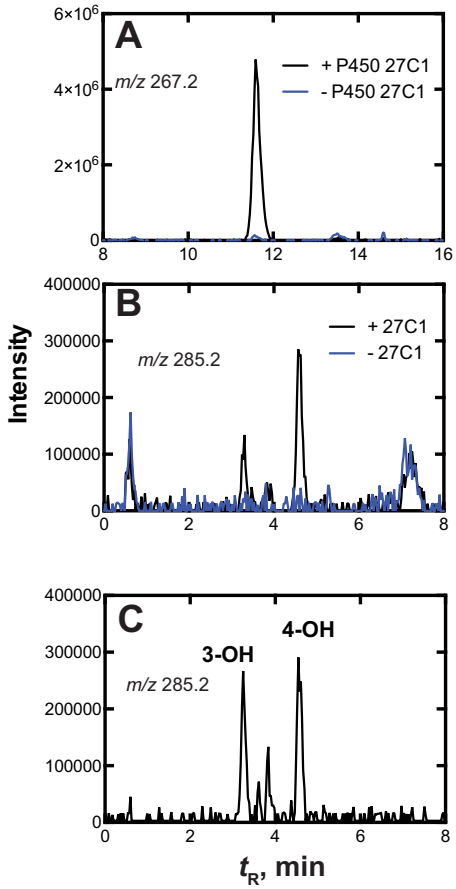

Figure 6. LC-MS chromatograms of oxidation products of all-*trans*-retinol. Shown is the detection of oxidation products of all-*trans*-retinol in the presence and absence of human P450 27C1. Reaction mixtures containing 10 μM all-*trans*-retinol, 5 μM Adx, 0.2 μM AdR, and 30 μM L-α-dilauroyl-*sn*-glycero-3-phosphocholine in 50 mM potassium phosphate buffer (pH 7.4) in the presence (*black line*) or absence (*blue line*) of 0.2 μM P450 27C1 were incubated with an NADPH-generating system at 37 °C for 5 min (2-ml reaction volume) (*A* and *B*). Reactions were quenched with *tert*-butyl methyl ether containing 20 μM butylated hydroxytoluene (1.0 ml), extracted following mixing with a vortex device, and concentrated under a nitrogen stream. Samples were analyzed by LC-MS. The extracted ion chromatograms are displayed: *m/z* 267.2 (desaturation) (*A*); *m/z* 285.2 (hydroxylation products) (*B*); *m/z* 285.2 for a separate mixture of 3-OH and 4-OH all-*trans*-retinol synthesized standards (*C*).

Reduction by Adx—Adx forms a complex with ADR and also has been known to be involved in electron delivery to mitochondrial P450s (45). Tight complexes with Adx have also been demonstrated with mitochondrial P450s 11A1 (12) and 11B1 (13), involving changes of low- to high-spin iron. However, we did not observe any spectral perturbation of P450 27C1 by the addition of Adx (in the absence or presence of equimolar amounts of all-*trans*-retinol), although the P450 27C1 activity is clearly dependent upon Adx for electrons (data not shown).

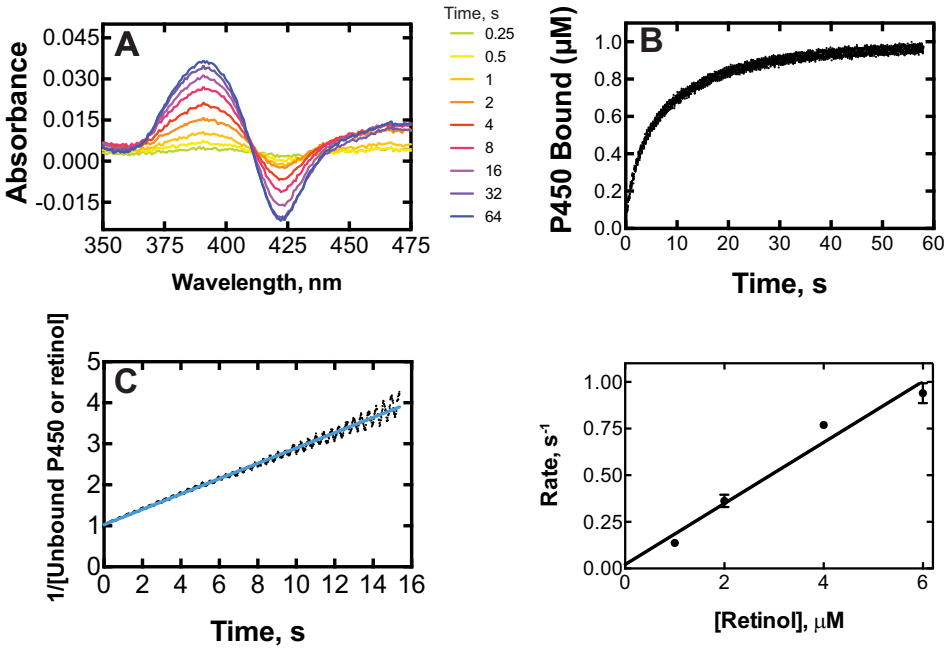

Figure 7. Binding of *all-trans*-retinol to P450 27C1. The assay was done in a stopped-flow spectrophotometer by mixing the contents of two syringes. One contained 2 μM P450 27C1 and 60 μM L-α-dilauroyl-*sn*-glycero-3-phosphocholine in 0.2 M potassium phosphate buffer (pH 7.4). The other contained 2 μM all-*trans*-retinol (*A–C*) and 60 μM L-α-dilauroyl-*sn*-glycero-3-phosphocholine in 0.2 M potassium phosphate buffer (pH 7.4). *A*, spectra collected over 64 s (with 64 spectra s^{-1} signal averaging). Reaction times are shown at the *right* (in seconds). *B*, kinetic traces of $\Delta A_{390} - A_{425}$, corrected to final P450 concentration. *C*, the data (*A* and *B*) were used to estimate a second-order rate of 1.9×10^5 M^{-1} s^{-1} by plotting the reciprocal of the free P450 concentration (*B*) *versus* time (42) (at 37 °C). *D*, similar experiments using P450 (1 μM final) and varying concentrations of all-*trans*-retinol and P450 (1 μM final concentration) was performed (at 37 °C), and the rates were calculated as a first-order process (42) using SVD fitting and plotted (means ± S.D. (*error bars*), n = 3–7) as a function of substrate concentration to estimate a second-order rate of 1.6×10^5 M^{-1} s^{-1} (slope) and $k_{off} = 0.022$ s^{-1} (y axis intercept) ($K_d = k_{off}/k_{on} \cong 130$ nM).

Preliminary assays were done by mixing photoreduced Adx with ferric P450 27C1 under an anaerobic CO atmosphere (supplemental Fig. S7). Considerable evidence for Adx acting as a mobile electron carrier has been published with another mitochondrial P450, P450 11A1 (13). In our experiments, the estimated rate of reduction (at 23 °C) was 1.3 ± 0.3 min^{-1} in the absence of the substrate retinol and 3.6 ± 0.3 min^{-1} in the presence of 5 μM retinol. We concluded that the presence of the substrate enhanced the rate of reduction, and further measurements were all done in the presence of substrate.

In a system with a 1:10:1 molar ratio of ADR/Adx/P450 27C1, the rate of reduction (in the presence of retinol) was 21 ± 1 min^{-1} at 37 °C (Fig. 8). (Rates of reduction of ADR by NADPH and Adx by ADR have been measured previously (32 and 5.4 s^{-1}, respectively, at 15 °C (21)). (In the steady-state kinetic assays, the enzymes were much less concentrated than in these anaerobic experiments, with 7.5-fold less ADR, 3-fold less Adx, and 75-fold less P450.)

Product release—A trapping assay was used in which a 1:1 molar mixture of 2 μM P450 27C1 and dehydroretinol was mixed with 20 μM ketoconazole (see above). A first-order rate of 54 ± 5 min^{-1} was estimated for the release of the product dehydroretinol at 23 °C.

Another important approach to determining whether a step following product formation is rate-limiting is to establish whether or not there is a kinetic burst (43). When we extrapolated to time 0, no burst was seen (Fig. 9). We conclude that neither product release nor any step following product formation is rate-limiting.

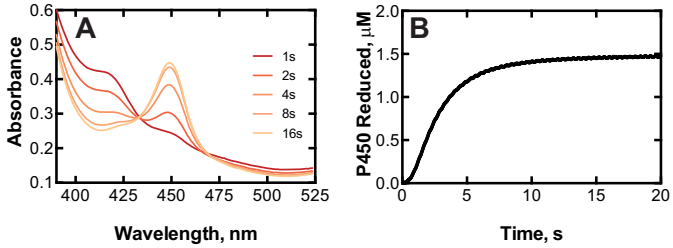

Figure 8. Reduction of P450 27C1 by Adx in the presence of ADR and NADPH. The assay was done anaerobically, under a CO atmosphere, by mixing the contents of two syringes in a stopped-flow spectrophotometer at 37 °C. One syringe contained 3 μM P450 27C1, 30 μM Adx, and 3 μM ADR. The other syringe contained 0.40 mM NADPH. Both syringes contained 200 mM potassium phosphate buffer (pH 7.4), 62 milliunits ml^{-1} protocatechuate dioxygenase, and 0.25 mM 3,4-dihydroxybenzoic acid. *A*, scans (375–525 nm) were collected over 20 s. *B*, kinetic trace of P450 reduction (measured difference $A_{446} - A_{412}$). The data were fit as a first-order process (42) using SVD fitting to obtain a rate (mean of 13 experiments ± S.D.) of 21 ± 1 min^{-1}.

KIEs

Deuterated retinols were synthesized (with >95% atomic excess; see supplemental material, including supplemental Fig. S6) and used to test the hypothesis that C–H bond breaking is a rate-limiting step in the desaturation or hydroxylation of retinol. We do not have information about the stereospecificity of hydrogen abstraction from retinol (which is pro-chiral at C-3 and C-4), so the dideuterated retinol derivatives 3,3-d_2 and 4,4-d_2 retinol were prepared, as well as tetradeuterated 3,3,4,4-d_4 retinol. (The synthesized 4,4-d_2 and 3,3,4,4-d_4 retinols also had deuterium at the side chain carbinol position (C-15), but this is irrelevant in the assays in that no oxidation occurs there.)

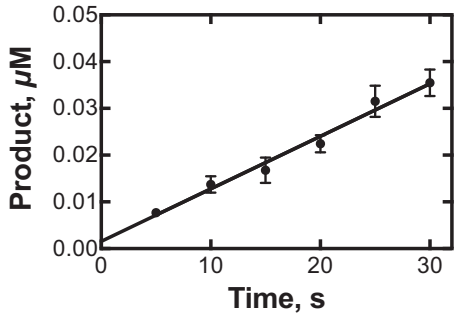

Figure 9. Lack of a kinetic burst of product (dehydroretinol) formation by P450 27C1. Time course assay of all-*trans*-retinol desaturation with linear extrapolation to time 0, providing evidence for lack of burst kinetics. Reaction mixtures contained 0.02 μM P450 27C1, 5 μM Adx, 0.2 μM AdR, 30 μM L-α-dilauroyl-*sn*-glycero-3-phosphocholine, and 20 μM *all-trans*-retinol in 100 mM potassium phosphate buffer (pH 7.4) and were incubated in the presence of an NADPH-generating system at 37 °C for 5–30 s. Reactions were quenched with *tert*-butyl methyl ether containing 20 μM butylated hydroxytoluene and analyzed by UPLC with UV detection. *Error bars*, S.D.

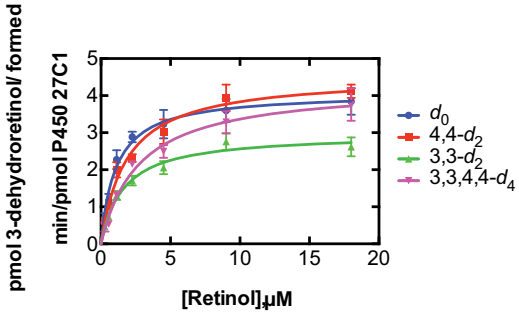

Figure 10. KIEs for all-*trans*-retinol desaturation. Steady-state kinetics of all-*trans*-retinol and deuterated all-*trans*-retinol desaturation by human P450 27C1. Reaction mixtures (0.5 ml) containing 0.02 μM P450, 5 μM Adx, 0.2 μM AdR, and 30 μM L-α-dilauroyl-*sn*-glycero-3-phosphocholine in 50 mM potassium phosphate buffer (pH 7.4), with varying amounts of substrate, were incubated in the presence of an NADPH-generating system at 37 °C for 2 min. Reactions were quenched with 1.0 ml of *tert*-butyl methyl ether containing 20 μM butylated hydroxytoluene, and the products were analyzed by UPLC/UV. Steady-state parameters were estimated using hyperbolic (nonlinear regression, with estimated internal S.D. (*error bars*)) in GraphPad Prism as follows: with d_0-retinol, $k_{cat} = 4.1 \pm 0.2$ min^{-1}, $K_m = 1.1 \pm 0.2$ μM, $k_{cat}/K_m = 3.7 \pm 0.7$ μM^{-1} min^{-1} (*blue line*); with 4,4-d_2 retinol, $k_{cat} = 4.5 \pm 0.2$ min^{-1}, $K_m = 1.8 \pm 0.3$ μM, $k_{cat}/K_m = 2.5 \pm 0.4$ μM^{-1} min^{-1} (*red line*); with 3,3-d_2 retinol, $k_{cat} = 3.0 \pm 0.2$ min^{-1}, $K_m = 1.6 \pm 0.3$ μM, $k_{cat}/K_m = 1.8 \pm 0.4$ μM^{-1} min^{-1} (*green line*); with 3,3,4,4-d_4 retinol, $k_{cat} = 4.3 \pm 0.3$ min^{-1}, $K_m = 2.7 \pm 0.6$ μM, $k_{cat}/K_m = 1.6 \pm 0.4$ μM^{-1} min^{-1} (*pink line*).

The KIE experiment that is most informative about a rate-limiting step is a noncompetitive intermolecular design, in which k_{cat} and K_m are measured with varying concentrations of protiated and deuterated substrates and used to calculate ^{D}V and $^{D}(V/K)$, defined as $^{H}k_{cat}/^{D}k_{cat}$ and $(^{H}k_{cat}/^{H}K_m)/(^{D}k_{cat}/^{D}K_m)$, respectively, with H and D indicating parameters measured with protium and deuterium at a site (1, 46, 47).[4]

Relatively small but reproducible changes were observed in the rates of desaturation when using deuterium-labeled substrates; low KIEs were observed for desaturation with 3,3-d_2, 4,4-d_2, and 3,3,4,4-d_4 retinol (Fig. 10). Most significantly, a KIE of ~2 ($^{D}(V/K)$) was observed when deuteriums were present at C-3 of the substrate (3,3-d_2 and 3,3,4,4-d_4), whereas the $^{D}(V/K)$ for 4,4-d_2 retinol was calculated to be only ~1.5.

In a separate experiment, we quantitated the levels of 3- and 4-hydroxylation of the deuterium-labeled substrates by P450 27C1 using LC-MS (Fig. 11). We found that 3-hydroxylation was significantly increased (3.7-fold) when deuterium atoms were present at C-4 (4,4-d_2 retinol). Conversely, when deuterium atoms were present at C-3 (3,3-d_2 retinol), 3-hydroxylation was strongly attenuated (apparent KIE 9.4, based on activity at a single substrate concentration). In both cases, the level of 4-hydroxylation remained relatively unchanged.

We considered the possibility that deuterium scrambling might occur after abstraction of a hydrogen atom from C-3 via a radical intermediate (or, alternatively, from a carbocationic intermediate that might be formed from further electron transfer (37)) (Fig. 2). Accordingly, we analyzed the desaturation and 4-hydroxylation products of 4,4-d_2 retinol by LC-HRMS. The masses detected at 100,000 resolution were consistent with those of the expected products, providing evidence against migration of deuterium from the C-4 to the adjacent C-3 site (Fig. 12).

Discussion

We have established that P450 27C1 is located in the skin, is involved in the desaturation of retinol, and also forms minor amounts of 3-OH and 4-OH retinol. Within the catalytic cycle, the reduction of ferric iron and C–H bond-breaking steps both contribute to limiting the reaction rates, but substrate binding and product release do not.

Skin is a major organ, in terms of collective body mass, and metabolism there is of interest with many drugs (applied cutaneously) and with a number of endogenous chemicals. Regarding P450s, there is some evidence that P450s 1A1, 1A2, 1B1, 2A6, 2B6, 2C18, 2C19, 2D6, 2E1, 2J2, 2R1 2S1, 2U1, 2W1, 3A4, 3A5, 4B1, 4F2, 4F3, 4F22, 11A1, 17A1, 24A1, 26A1, 26B1, 26C1, 27A1, and 51A1 are expressed in human skin samples or in derived cells (in culture) (48–54). However, almost all of the data are at the mRNA level. Only in a few cases has protein expression been reported, and then only at the immunohistochemical or enzyme activity level (52, 54). Previous studies by Törmä and Vahlquist (41) demonstrated the presence of retinol 3,4-desaturation activity in human skin epidermis, as well as in human keratinocytes, melanoma cells, and HeLa cells (55). In the present study, we identified P450 27C1 in human skin samples using proteomic and immunochemical methods (Figs. 3–5) but did not find P450 27C1 in the human liver and kidney samples that we analyzed (Fig. 4, *B* and *C*). Earlier studies with an oligonucleotide probe selective for P450 27C1 (compared with P450s 27A1 and 27B1) indicated the presence of P450 27C1 mRNA in several human tissues, including the liver, kidney, and pancreas (23). Skin mRNA had not been included in that study. One possibility for the apparent difference in tissue localization is that the oligonucleotide probe used previously (23) was not specific, although that seems unlikely in the context of the selectivity demonstrated *versus* P450 27A1 and 27B1 sequences. An alternative possibility is that mRNA is formed in several tissues but not translated into protein, which would not be surprising in light of the overall concordance between mRNA and protein expression (56). The possibility also exists that the mRNA could be alternatively spliced or transcribed in

[4] The conventions $^{D}V = {}^{H}k_{cat}/{}^{D}k_{cat}$ and $^{D}(V/K) = ({}^{H}k_{cat}/{}^{H}K_m)/({}^{D}k_{cat}/{}^{D}K_m)$ of Northrop (1) are used for KIEs.

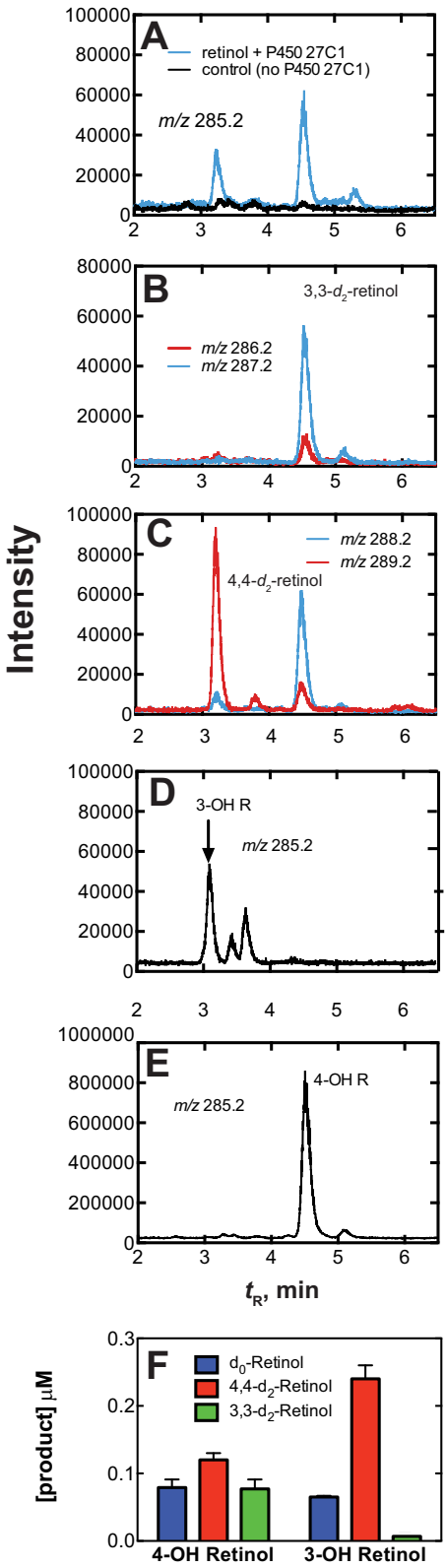

Figure 11. Effects of deuterium on formation of 3- and 4-OH retinol. Shown is detection of hydroxylation products of 3,3-d_2 and 4,4-d_2 retinol by P450 27C1. Reaction mixtures containing 7 μM specified all-*trans*-retinol, 0.2 μM P450 27C1, 5 μM Adx, 0.2 μM AdR, and 30 μM L-α-dilauroyl-*sn*-glycero-3-phosphocholine in 50 mM potassium phosphate buffer (pH 7.4) were incubated in the presence of an NADPH-generating system at 37 °C for 5 min (2-ml reaction volume). Reactions were quenched with *tert*-butyl methyl ether containing 20 μM butylated hydroxytoluene, extracted following mixing with a vortex device, and concentrated under a nitrogen stream. Samples were analyzed by LC-MS. Displayed are extracted ion chromatograms of the following: *m/z* 285.2 all-*trans*-retinol reacted in the presence (*blue line*) or absence (*black line*) of P450 27C1 (*A*); *m/z* 286.2 (*red line*; 3-OH) and *m/z* 287.2 (blue line, 4-OH) products of 3,3-d_2 retinol (*B*); *m/z* 288.2 (*blue line*, 4-OH) and *m/z* 289.2 (*red line*, 3-OH) products of 4,4-d_2 retinol (*C*); *m/z* 285.2 3-OH all-*trans*-retinol standard (*D*); and *m/z* 285.2 4-OH all-*trans*-retinol standard (*E*). *F*, concentrations of OH retinol products formed from protiated and deuterated retinol substrates ($n = 3$, means ± S.D. (*error bars*)).

other tissues. In reviewing the Human Protein Atlas (http://www.proteinatlas.org),[3] the highest level of mRNA expression of CYP27C1 is in skin (57). Some other sites in which higher than baseline levels were seen include the uterine cervix, urinary bladder, and vagina (57). Trace but apparently real levels of CYP27C1 mRNA were found in many other tissues, including those that we reported previously (23). Our conclusion is that we were observing these low levels of expression in our earlier data (23), which was misleading in that skin was not included.

Although expression in retinal epithelium is critical in the biology of dehydroretinol in fish (24), the literature does not indicate the presence of dehydroretinoids (vitamin A_2) in human eyes (57). 3,4-Dehydroretinoic acid is also formed by human P450 27C1 (25), but the biological activities of retinoic acid and 3,4-dehydroretinoic acid are similar in human keratinocytes (58). In human skin, dehydroretinol accounts for ~25% of the retinoid pool (59, 60), but the function remains unknown. Levels of dehydroretinol are elevated in psoriasis (60) and squamous cell carcinoma and keratocanthoma (61), and the desaturation activity is induced by exposure to UVA/B light (62). In our analyses, the levels of the two forms of P450 27C1 only varied ~2-fold among the five human samples analyzed (Fig. 4*A*). This level of variation is similar to that commonly seen for P450s involved in normal physiological processes (63) and differs from the wide variation in levels of the P450s that are involved in the metabolism of xenobiotic chemicals (5, 63).

We utilized the original human *CYP27C1* sequence (GenBank™ AC027142; March 28, 2000) (Fig. 5) in consideration of what is actually expressed in human skin. The Uniprot Q4G0S4 372-residue sequence is clearly wrong. No P450 this short has ever been identified to our knowledge, even in bacteria, and it would not be expected to be catalytically active. The 482-amino acid version that we expressed (25) and used in catalytic assays (Figs. 6–9) is similar in M_r to the smaller protein found in the skin (Fig. 4*A*). The larger protein (Fig. 4) contained the peptides that correspond to residues 1–537 (Fig. 5*A*), in that the peptides for residues 1–11 and 524–537 were characterized. The smaller protein contains residues 70–78 (Fig. 5*B*), so this peptide must be near the N terminus, but we cannot determine exactly where P450 27C1 was cleaved. We presume that the smaller protein is catalytically active, in that its size is similar to that of the recombinant protein (Fig. 4*A*). Which of these proteins is present in mitochondria is currently unknown. The program MitoFATES (64) (mitf.cbrc.jp/MitoFates/cgi-bin/top.cgi)[3] predicts a TOM20 recognition motif at residues 9–14 and an MPP cleavage site at residue 66, the latter of which is what we had serendipitously designed in our original *Escherichia coli* expression construct, leaving an N terminus similar to that observed for murine P450 27B1 (23). Further work is needed, however, to characterize the transport of a specific sequence into mito-

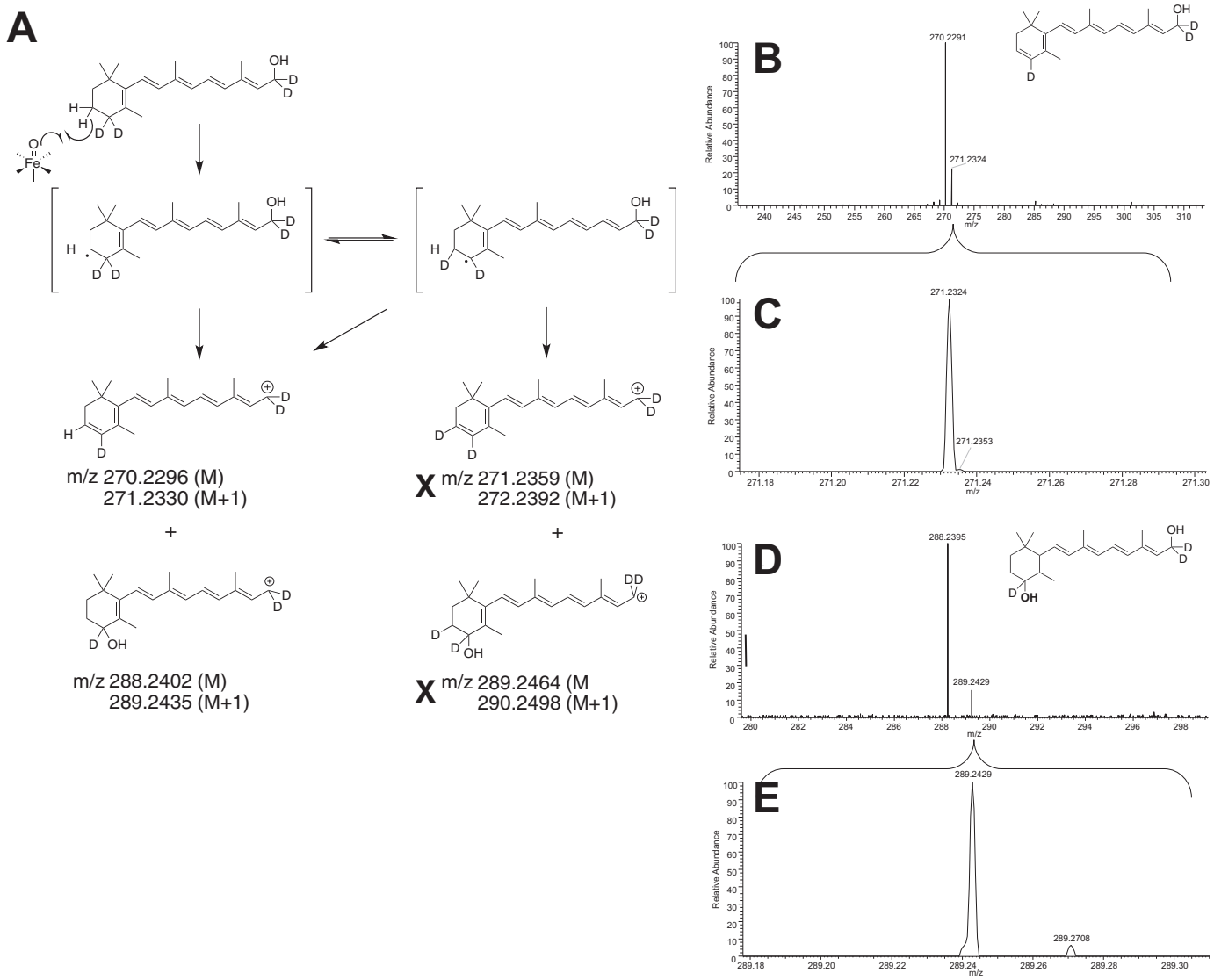

Figure 12. HRMS of 4,4-d_2 retinol oxidation products formed by P450 27C1. Shown is analysis of desaturation and 4-hydroxylation products of 4,4-d_2 retinol by P450 27C1. Reaction mixtures containing 0.2 μM P450 27C1, 5 μM Adx, 0.2 μM AdR, 30 μM L-α-dilauroyl-*sn*-glycero-3-phosphocholine, and 10 μM 4,4-d_2 retinol in 50 mM potassium phosphate buffer (pH 7.4) were incubated in the presence of an NADPH-generating system at 37 °C for 5 min (2-ml reaction volume). Reactions were quenched with *tert*-butyl methyl ether containing 20 μM butylated hydroxytoluene, extracted following mixing with a vortex device, and concentrated under a nitrogen stream. *A*, scheme of possible events. Those shown not to occur are indicated (×). Samples were analyzed by LC-HRMS. The relevant segments of the spectra are shown for 3,4-dehydroretinol (*B*) (*C* shows an expansion of *B*) and 4-OH retinol (*D*) (*E* shows an expansion of *D*).

chondria. Our current results indicate the methionine at residue 1 as the start site for protein translation (Fig. 5*A*).

Desaturation is a relatively infrequent event in P450 oxidations, at least compared with hydroxylation, and we were interested in defining rate-limiting steps. Very little work has been published on rate-limiting steps in reactions by the seven mitochondrial P450s (11A1, 11B1, 11B2, 24A1, 27A1, 27B1, and 27C1), including KIE studies (5, 65). The literature indicates that the KIEs observed for some microsomal P450 desaturation reactions are relatively high (33, 66), depending on the experimental design. We measured ^{D}V and $^{D}(V/K)$, the latter of which is considered the most useful KIE experiment to establish to what extent C–H bond breaking is rate-limiting in a reaction (1, 46, 47). The KIE values are relatively low, in terms of the values seen in some (but certainly not all) P450 oxidations (47), but nevertheless the KIE values are significantly greater than unity, indicating some contribution to rate limitation.

Several other steps in the catalytic cycle were also measured. The rate of substrate binding was measured to be $1.6–1.9 \times 10^5$ M^{-1} s^{-1}, using two approaches (Fig. 7). The reaction appeared to be monophasic but is slow in terms of what is expected for a diffusion-limited reaction (67). Further, the apparent rate constant is at least 1 order of magnitude less than those measured for substrate/ligand binding to some human microsomal P450s (68–70) and bacterial P450 101A1 ($P450_{cam}$) (71). The slower rate measured for P450 27C1 may reflect the existence of a slow step, following initial binding, that leads to the spin state change, as in the case of P450 3A4 (69, 72). Regardless, substrate binding and product release are considerably faster than the overall oxidation, and the absence of burst kinetics already indicates that a step following product formation cannot be rate-limiting (Fig. 9). The rate of reduction of ferric P450 27C1 is somewhat faster than overall catalysis (Fig. 8), and we propose that it can contribute in part as a rate-limiting step. Preliminary

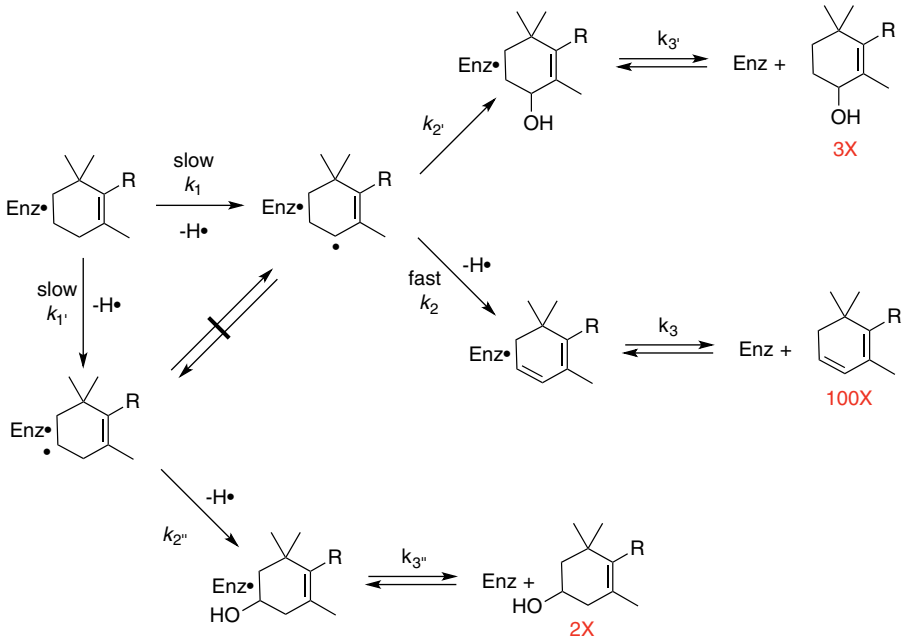

Figure 13. Mechanistic relationship of retinol 3- and 4-hydroxylation to desaturation. The conclusions are based on the results of KIE and deuterium labeling studies. For more details, see "Discussion."

analysis of a simplified KinTek Explorer® mechanism (supplemental Fig. S8) indicated that the simulated rate of the overall reaction was increased when the rate constant for the reduction step was raised above the rate observed in our work, in support of the view that the reduction of ferric P450 27C1 is a partially rate-limiting step. The reduction rate was stimulated in the presence of the substrate retinol (~3-fold) (supplemental Fig. S7); sometimes P450 reduction rates are stimulated by substrates and sometimes not (73). It is of interest to note that Tuckey *et al.* (19) concluded that the reduction of mitochondrial P450 11A1 by Adx was rate-limiting in human placenta, as well as in reconstituted systems (74). To our knowledge, of the seven mitochondrial P450s, only with P450 11A1 has a ferrous-O_2 complex been characterized (and at low temperature) (17). We attempted to characterize such a P450 27C1 complex by mixing photoreduced P450 27C1 with O_2 but were not successful. It would be desirable to measure the rate of Adx reduction of this complex, but no such mitochondrial P450 reaction has been characterized in detail yet.

The KIE values for desaturation (Fig. 10) and 4-hydroxylation are relatively low. We have not estimated the intrinsic KIE, ^{D}k, in either case but suspect that it may be considerably higher. Thus, the values of 1.5–2.3 we measured for $^{D}(V/K)$ (Fig. 10) may be attenuated due to the tight binding of retinol (previously estimated K_d of 5.6 nM (24) and k_{off} of 1 min^{-1} (this work)). This represents a case of high forward commitment to catalysis (C_f, using the conventions of Northrop (1) and as elaborated by Northrop (1) and elsewhere (47)),

$$^{D}(V/K) = \frac{^{D}k + C_f}{1 + C_f} \qquad \text{(Eq. 1)}$$

(when there is no commitment to reverse catalysis). Thus, although it might not be intuitive, raising C_f (*i.e.* decreasing the substrate k_{off}) lowers the observed $^{D}(V/K)$ value for a reaction such as a P450-catalyzed oxidation, which is essentially irreversible. Therefore, the $^{D}(V/K)$ values measured here are probably lower than the ^{D}k and may not reflect a higher KIE.

The KIE and other deuterium experiments provide some insight into steps associated with the oxidation of retinol (Figs. 10, 11, and 13). We propose that abstraction of a C-4 hydrogen atom is the first step in both 4-hydroxylation and desaturation, in that both processes had low KIEs (Fig. 10). 3-Hydroxylation is a separate reaction and begins with abstraction of a C-3 hydrogen atom. This is an unfavorable reaction, possibly because, unlike the C-4 abstraction, it does not yield an allylic radical. The measured KIE values were much higher, and hydrogen atom abstraction is clearly rate-limiting for the minor 3-hydroxylation reaction (Fig. 11*F*). We were unable to measure a K_d for binding of the product dehydroretinol to P450 27C1, but the measured k_{off} rate was 50 min^{-1}, and no burst kinetics were seen (Fig. 10). HRMS results indicate that the 3- and 4-position radicals do not equilibrate (Fig. 13). The "metabolic switching" to yield more 3-OH retinol takes place with the substrate, not the C-4 allylic radical. In other words, slowing C-4 radical formation yields more retinol for the C-3 abstraction. C-3 abstraction is a minor pathway and, accordingly, not substantial enough to yield a noticeable shift to 4-hydroxylation or desaturation. Apparently, C-3 hydrogen abstraction is slower than Adx reduction. In the C-4 pathways, Adx reduction is slow enough to contribute to reaction rate limitation.

As mentioned earlier, it is unusual for a mammalian P450 to catalyze primarily desaturation instead of hydroxylation. Some examples of substrates that are primarily hydroxylated by P450s but also desaturated to some extent include valproic acid, warfarin, lauric acid, lovastatin, ethyl carbamate (urethane), testosterone, bufuralol, ezlopitant, and capsaicin (32, 34–36, 75, 76). However, P450s catalyzing predominantly only desaturation are known in plants (28, 29) and yeasts (30, 31). Non-heme

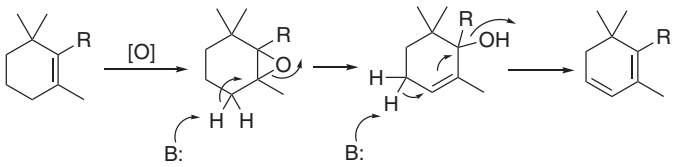

Figure 14. An alternative mechanism for retinol desaturation. For more details, see "Discussion."

desaturases are important in oxidation of fatty acids and some other alkanes, and a few residues have been shown to alter the balance of desaturation and hydroxylation (27, 77, 78). Some mammalian P450s are also capable of (ω-)desaturation of fatty acids (34).

The bifurcation of desaturation and hydroxylation has also been considered at a theoretical level (27, 37, 38). Kumar *et al.* (37) concluded that desaturation involved carbocationic intermediates, generated by further electron transfer from an initial carbon radical. Desaturation is proposed to occur because of stereoelectronic inhibition of the oxygen rebound process (37). The conclusion that desaturation occurs only through a carbocationic intermediate (37) may or may not be correct, and our results do not address this issue directly. It is of interest to note, however, that no shifts of the 3- or 4-deuterium atoms were observed (Fig. 12). This lack of allylic scrambling does not necessarily negate the hypothesis about carbocations. Ji *et al.* (38) did not consider carbocations but concluded that the difference in O–H *versus* C–O bonds formed is critical in the outcome, and Cooper *et al.* (27) also favored a radical mechanism instead of carbocationic. This is concluded to be important, and π-conjugation, which occurs in the desaturation of retinol, lowers the excitation energy. In these theoretical papers (37, 38), the difference between hydroxylation and desaturation can ultimately be rationalized in the context of the structure of the enzyme–substrate complex.

One alternative mechanism of desaturation that can be considered is shown in Fig. 14, in which the initial reaction is an epoxidation of the cyclohexenyl ring, followed by two base-catalyzed abstractions of the C-3 and C-4 hydrogens. This mechanism could be consistent with all of our data on isotope effects, and there is no single experiment that we have done that would rule this out. We are inclined against this mechanism in that the epoxide would be expected to be relatively stable, as in the case of cyclohexene oxide (79) and vitamin K epoxide (80). Additionally, we did not find any additional LC-MS peaks with *m/z* 285 (Fig. 6). If this were the mechanism, then the hydroxylation reactions would be separate events, not as shown in Fig. 13, and discussion of competition between hydroxylation and desaturation would be a moot point.

The effect of limited changes in amino acids on the partitioning between desaturation and hydroxylation has been appreciated in non-heme iron monooxygenases for some time (77, 78). A similar balance has been observed in two bacterial P450s (102A1 and 199A4) by Whitehouse *et al.* (39) and Bell *et al.* (40), respectively, in which a 5-amino acid change in P450 102A1 or a single-amino acid change in P450 199A4 (F185V) could change the ratio of hydroxylation to desaturation. Although no three-dimensional structure of a P450 27C1-retinoid complex is available yet, we believe that it might be instructive as to the proclivity toward desaturation and suggest specific site-directed mutagenesis experiments.

In summary, we have characterized several aspects of human P450 27C1, a retinol desaturase found in skin. The enzyme also catalyzes 3- and 4-hydroxylation as minor events, and the balance of these reactions is probably due to the allylic nature of the reaction and to the juxtaposition of the substrate in the active site. Small but significant deuterium KIEs were calculated, and metabolic switching of minor products was observed, leading us to conclude that abstraction at C-4 may occur first. Rate limitation at other key steps in P450 oxidation of retinol was considered, including substrate binding and product release, as well as reduction. We conclude that at least two reaction steps, C–H bond breaking and Adx reduction of the ferric enzyme, contribute to limiting rates of the desaturation of retinol by P450 27C1.

Experimental procedures

Chemicals

4-Oxo (keto) retinoic acid methyl ester was prepared as described previously (24). All-*trans*-retinol, zeazanthin, retinol acetate, retinol palmitate, and 3,4-dihydroxybenzoic acid were obtained from Sigma-Aldrich. 3,10-Dimethyl-5-dezaflavin was purchased from Sinova (Bethesda, MD) and dissolved in *N*,*N*-dimethylformamide for use in photoreduction experiments (81).

Chemical synthesis

The synthesis and characterization of 3-OH-all-*trans*-retinol, 4-OH-all-*trans*-retinol, and 3,3-d_2, 4,4-d_2-, and 3,3,4,4-d_4-all-*trans*-retinol are described in detail in the supplemental material.

Enzymes

Human P450 27C1 (23, 25) and bovine Adx and ADR (24, 82, 83) were expressed in *E. coli* and purified as described previously (supplemental Fig. S1).

For the preparation of antibodies, the P450 27C1 was further purified to remove some trace contaminants. The P450 27C1 fraction eluted from the Ni^{2+}-NTA column (23) was supplemented with 0.2% (w/v) Emulgen 913, dialyzed against 10 mM potassium phosphate buffer (pH 7.4) containing 20% glycerol (v/v) and 0.2% (w/v) sodium cholate, and then passed through a DEAE column (DEAE-Sepharose Fast Flow, GE Healthcare) equilibrated with 10 mM potassium phosphate buffer (pH 7.4) containing 20% glycerol (v/v), 0.2% (w/v) sodium cholate, and 0.2% (w/v) Emulgen 913. The void fraction, containing P450 27C1, was analyzed by SDS-PAGE for impurities, and the highest purity protein fractions were loaded onto a hydroxylapatite column equilibrated with 10 mM potassium phosphate buffer (pH 7.4) containing 20% glycerol (v/v). The column was washed extensively with the same buffer to remove residual detergent. Highly purified P450 27C1 was eluted with 500 mM potassium phosphate buffer (pH 7.4) containing 20% glycerol (v/v). The protein concentration was estimated using a bicinchoninic acid (BCA) assay (Bio-Rad). The protein was dialyzed against PBS (15 mM potassium phosphate buffer (pH 7.4) containing 0.15 M

NaCl) for polyclonal antibody development in rabbits (see below). Protocatechuate 3,4-dioxygenase (*Pseudomonas* sp.) was purchased from Sigma-Aldrich.

Tissue samples

All work was done with the approval of the Vanderbilt institutional review board, which considers these particular studies exempt if sample donors are not identified. The human liver and kidney samples were obtained through the Nashville Regional Organ Procurement Agency. Two human skin samples, from the abdominal area of an adult male (sample W, code A16-6) and female (sample P, code A16-4), were obtained from Prof. Joseph Corbo (Washington University School of Medicine, St. Louis, MO) (these were used in Fig. 4). A third sample, from the breast area of an adult male, was also obtained from the same source and used in the work presented in Fig. 3. Three other skin samples (all from adult female breast) were obtained from the tissue procurement source at Vanderbilt University Medical Center and are coded 37, 51, and 57 (these were used in Fig. 4, along with samples W and P from Washington University). The identities of the individuals were not disclosed.

Tissue samples were homogenized using a two-step procedure. The first step was done with an IKA disperser homogenizer (on ice) (4 × 10 s). The resulting mixture was then processed with a motorized glass-Teflon Potter-Elvehjem tissue homogenizer (on ice) (4 × 15-s pulses, with ~4 up-and-down strokes during each). Approximately 400 mg of human liver and kidney was homogenized in 10 ml of 50 mM potassium phosphate (pH 7.4) buffer. Much more disruptive methods were required for human skin samples: ~400 mg of human skin was homogenized in 6 ml of lysis buffer (6 M urea, 2 M thiourea, 4% (w/v) sodium CHAPS (w/v), 0.1% SDS (w/v)). Unhomogenized skin tissue was filtered out through glass wool, and the homogenates were centrifuged at 2,000 × *g* for 10 min, and the resulting supernatant was centrifuged at 16,000 × *g* for 20 min (at 4 °C). The supernatant was collected and precipitated with 5 volumes of cold acetone and chilled overnight at −20 °C. The precipitated proteins were pelleted at 16,000 × *g* for 20 min (at 4 °C), washed once with chilled 50% acetone (aqueous) with vortex mixing, and centrifuged again at 16,000 × *g* for 10 min. The resulting pellets were resuspended in 50 mM Tris buffer (pH 7.4) containing 2% SDS (w/v) and heated at 95 °C for 5 min. The concentrations of protein in all tissue samples were estimated using a BCA assay (Bio-Rad) or Pierce 660-nm protein assay (with detergent compatibility reagent) (Thermo Fisher Scientific).

Antibodies

Rabbit antibodies were raised by Cocalico Biologicals (Stevens, PA). Three rabbits were immunized with a total of 6 mg of purified P450 27C1 (see above; further purified by by DEAE and hydroxylapatite chromatography to remove some impurities). The rabbits were injected with purified protein in PBS, followed by three boosts over a period of 49 days. A test bleed was collected, and antibody strength was tested using an immunoblot with purified P450 27C1 as an antigen. Unless further boosting was required for more antibody production, the rabbits were then boosted a final time before exsanguination. The sera were compared, and the best serum was used based on specificity and titer.

Rabbit anti-27C1 antibody was purified by affinity chromatography with purified recombinant protein (84). Purified 27C1 was coupled to CNBr-activated Sepharose (GE Healthcare) according to the manufacturer's instructions. The coupled beads were incubated with diluted antiserum from rabbit number 497 (1:10 dilution in PBS, v/v) at room temperature overnight with end-over-end rotation. The suspension was washed extensively with PBS until the A_{280} was <0.01. Bound antibody was eluted with 0.20 M glycine-HCl buffer (pH 2.5) in 1-ml fractions and neutralized with 1.0 M Tris-HCl buffer (pH 8.0). Fractions containing antibody (monitored by A_{280} measurements) were combined, and protein concentration was measured using a BCA assay (Pierce/Thermo Fisher Scientific).

Immunoblotting (Western blotting) of tissue homogenates was carried out using the purified 497 antibody and reagents purchased from LI-COR (Lincoln, NE). Proteins from skin (20 μg), liver (50 μg), and kidney (50 μg) were separated using SDS-polyacrylamide gel electrophoresis and then transferred to nitrocellulose membranes (85) and stained with SyPro Ruby Blot Stain (Thermo Fisher Scientific) for total protein visualization using a PharosFX Plus molecular imager (Bio-Rad). Higher protein loads of the skin homogenates led to poor resolution from the keratins. The membranes were blocked with LI-COR Odyssey blocking buffer. Immunoblots were optimized with a 1:200 dilution (v/v) of the immunopurified rabbit antiserum (~1 μg of protein/ml) and a $1:10^4$ dilution (v/v) of goat anti-rabbit 800CW near-infrared (IR) dye for the secondary antibody incubation (LI-COR protocol). Fluorescence signals were detected and quantified using a LI-COR Odyssey infrared imaging system (Thermo Fisher Scientific).

Proteomic analysis of skin homogenates

Proteins in the skin homogenate samples (prepared above) were separated by SDS-polyacrylamide gel electrophoresis (10% acrylamide, w/v), and bands were visualized with Coomassie SimplyBlue SafeStain (Thermo Fisher Scientific). Recombinant P450 27C1 was used to guide the selection of migration distances selected for analysis (the M_r is less because it is 58 residues shorter (23)) as well as immunoblots done on portions of the same gel (Fig. 4). The molecular weight region corresponding to recombinant P450 27C1 and the higher region, which was suspected to contain a higher-M_r P450 27C1 protein, was excised and processed for in-gel digestion. In-gel trypsin digestion was performed as described (86). Extracted peptides were analyzed on a nanoLC Ultra system (Eksigent Technologies, Dublin, CA) interfaced with an LTQ Orbitrap XL mass spectrometer (Thermo Fisher Scientific). Approximately 2 μg of peptides were reconstituted in 0.1% HCO_2H and pressure-loaded (1.5 μl min^{-1}) onto a 360-μm outer diameter × 100-μm inner diameter microcapillary analytical column packed with Jupiter octadecylsilane (C18) resin (3 μm, 300 Å; Phenomenex) and equipped with an integrated electrospray emitter tip. Peptides were then separated with a linear gradient composed of 0.1% HCO_2H in H_2O (solvent A) and 0.1% HCO_2H in CH_3CN (solvent B) as follows: 2% B held from 0 to 10 min and increased from 2 to 45% B from 10 to 55 min at 500 nl

min^{-1}. The spray voltage was set to 2.0 kV, and the heated capillary temperature was set to 200 °C. HCD MS/MS spectra were recorded in the data-dependent mode using a Top 2 method with an inclusion list containing *m/z* values corresponding to P450 27C1 tryptic peptides (Fig. 5) determined *in silico* with Skyline software (87). MS1 spectra were measured with a resolution of 70,000, an AGC target of 1e6, and a mass range from *m/z* 300 to 1,500. HCD MS/MS spectra were acquired with a resolution of 7,500, an AGC target of 1e5, and normalized collision energy of 35. Peptide *m/z* values that triggered MS/MS scans were dynamically excluded from further MS/MS scans for 20 s with a repeat count of 1. In some cases, a Q Exactive mass spectrometer (Thermo Fisher Scientific) was used for parallel reaction monitoring analysis. Tryptic peptides from the recombinant P450 27C1 protein were used to determine retention time windows to monitor for the skin homogenate. Retention time windows were set at ±1 min for each peptide in the C-terminal region. Peptides from the previously undetermined N-terminal region were monitored for the entirety of the LC gradient. MS1 spectra were measured with a resolution of 70,000, an AGC target of 3e6, and a mass range from *m/z* 300 to 1,500. HCD MS/MS spectra were acquired with a resolution of 17,500, an AGC target of 5e5, and NCE of 27. For C-terminal peptides, a maximum injection time of 200 ms was used with a loop count of 10. An isolation width of *m/z* 1.5 with an offset of *m/z* 0.1 was used. For N-terminal peptides, a maximum injection time of 120 ms was used with a loop count of 18. Skyline software (87) was used to monitor both precursors and products from the parallel reaction monitoring analysis. Raw data files were analyzed using MyriMatch (88) against a decoy protein database consisting of forward and reversed human Uniprot/Swissprot database (version 20160620). The precursor ion mass tolerance was 10 ppm, and the fragmentation tolerance was 20 ppm for the database search. Methionine oxidation (15.9949 Da, dynamic) and cysteine modifications by iodoacetamide (carbamidomethyl, 57.0214 Da, static) were searched as modifications. The maximum *Q* values of peptide spectrum matches were adjusted to achieve either a peptide or a protein false discovery rate <5% using IDPicker software (version 3.1.642.0) (89).

Spectroscopy

UV-visible absorbance spectra were recorded using OLIS/Cary 14 and OLIS/Aminco DW-2 spectrophotometers (On-Line Instrument Systems, Bogart, GA). Stopped-flow measurements were made with an OLIS RSM-1000 instrument operating in the rapid-scanning mode (1,000 spectra s^{-1}, with signal averaging for runs >4 s). In general, the slit widths were 1.24 mm (nominal 8-nm bandwidth), the gratings were 600 lines mm^{-1} (spectral width 300 nm), and the wavelength center was 450 nm. The temperature was controlled with a jacketed water bath and an external Jubalo F-25 circulating water bath (temperatures are noted for individual experiments). Collected spectra were analyzed with single-variable decomposition (SVD) software (OLIS Global Works) to estimate rates, using appropriate models in the manufacturer's software. The number of replicate traces and the S.D. are indicated for each experiment.

Anerobic kinetic experiments were conducted by loading the stopped-flow instrument with samples from tonometers that had been degassed and placed under a CO atmosphere as described in detail elsewhere (46, 90, 91). The syringes of the stopped-flow apparatus had previously been scrubbed with an anaerobic solution of a mixture of protocatechuate dioxygenase and 3,4-dihydroxybenzoic acid (92, 93).

Incubations with P450 27C1

Incubations were done at 37 °C in a shaking water bath. Typically, incubations for steady-state reactions were based on work done with other mitochondrial P450s and included 0.02 μM P450 27C1, 5 μM Adx, and 0.2 μM ADR in 50 mM potassium phosphate buffer (pH 7.4) (0.5-ml final volume) (25), along with varying concentrations of all-*trans*-retinol and an NADPH-generating system (94). All procedures with retinoids were done in amber glass vials under dim light because of the photosensitivity. Retinol was dissolved in ethanol, and the final concentration of ethanol in the reactions was ≤1% (v/v). We found that the presence of 30 μM L-α-dilauroyl-*sn*-glycero-3-phosphocholine did not enhance the initial reaction rate but yielded a longer period of linearity of product formation. Typical reactions were done for 2 min and quenched by the addition of 2 volumes of *tert*-butyl methyl ether containing 20 μM butylated hydroxytoluene (to prevent chemical oxidation). Samples were resuspended in 50% ethanol (aqueous, v/v) for chromatographic separation (100 μl).

Chromatography

HPLC with UV-visible absorbance detection was routinely used for measurement rates of oxidation of retinol in steady-state kinetic assays. Products were generally separated using a Waters Acquity UPLC system and an Acquity UPLC-BEH octadesylsilane (C18) column (50 mm × 2.1 mm, 1.7 μm) with a solvent system consisting of 4.9% CH_3CN, 0.1% HCO_2H, and 95% H_2O (solvent A) and 95% CH_3CN, 0.1% HCO_2H, and 4.9% H_2O (solvent B) (all v/v). Samples were injected with a 20-μl loop, and a linear gradient was used for analysis of 3,4-dehydroretinol: 60–66% B (v/v) over 10 min at a flow rate of 0.3 ml min^{-1}. For detection of all P450-dependent oxidation products the following was used: 40–45% B over 5 min followed by 60–66% (all v/v) over 10 min at a flow rate of 0.3 ml min^{-1}. Similar UPLC systems were used for mass spectrometry measurements for enzyme incubations.

LC-MS experiments for detection of retinol oxidation products

LC-MS analyses of retinol oxidation products were done with samples introduced following UPLC as described above. For detection of oxidized products, a Thermo LTQ mass spectrometer was used; for high resolution mass measurement, a Thermo LTQ-Orbitrap mass spectrometer was required at 100,000 resolution. In both cases, the mass spectrometer was operated in the atmosphere pressure chemical ionization (APCI) positive ion mode and was tuned with authentic all-*trans*-retinol. The tune settings are as follows: sheath gas flow rate, 40; auxiliary gas flow rate, 10; sweep gas flow rate, 0; capillary temperature, 300 °C; APCI vaporizer temperature,

350 °C; source voltage set to 6 kV; source current, 5 μA; capillary voltage, 10 V; tube lens, 55 V.

Author contributions—K. M. J. synthesized the retinoids and did all of the enzymatic assays. T. T. N. P. purified P450 27C1 and ADR, purified and characterized the antibody, and performed the immunoquantitation experiments. K. M. J. and M. E. A. did the proteomic analysis of P450 27C1 expression in tissues, with K. M. J. F. P. G. conceived the project, purified Adx, and did the anaerobic stopped-flow measurements with K. M. J. F. P. G. and K. M. J. wrote most of the manuscript.

Acknowledgments—Some of the mass spectrometry and proteomic work was supported in part by National Institutes of Health Grant P30 CA068485 (Vanderbilt-Ingram Cancer Center Support Grant).

References

1. Northrop, D. B. (1982) Deuterium and tritium kinetic isotope effects on initial rates. *Methods Enzymol.* **87,** 607–625
2. Rendic, S., and Guengerich, F. P. (2012) Contributions of human enzymes in carcinogen metabolism. *Chem. Res. Toxicol.* **25,** 1316–1383
3. Rendic, S., and Guengerich, F. P. (2015) Survey of human oxidoreductases and cytochrome P450 enzymes involved in the metabolism of xenobiotic and natural chemicals. *Chem. Res. Toxicol.* **28,** 38–42
4. Auchus, R. J., and Miller, W. L. (2015) P450 enzymes in steroid processing. In *Cytochrome P450: Structure, Mechanism, and Biochemistry*, 4th Ed. (Ortiz de Montellano, P. R., ed) pp. 851–879, Springer, New York
5. Guengerich, F. P. (2015) Human cytochrome P450 enzymes. In *Cytochrome P450: Structure, Mechanism, and Biochemistry*, 4th Ed. (Ortiz de Montellano, P. R., ed), pp. 523–785, Springer, New York
6. Sangar, M. C., Bansal, S., and Avadhani, N. G. (2010) Bimodal targeting of microsomal cytochrome P450s to mitochondria: implications in drug metabolism and toxicity. *Expert Opin. Drug Metab. Toxicol.* **6,** 1231–1251
7. Avadhani, N. G., Sangar, M. C., Bansal, S., and Bajpai, P. (2011) Bimodal targeting of cytochrome P450s to endoplasmic reticulum and mitochondria: the concept of chimeric signals. *FEBS J.* **278,** 4218–4229
8. Mast, N., Annalora, A. J., Lodowski, D. T., Palczewski, K., Stout, C. D., and Pikuleva, I. A. (2011) Structural basis for three-step sequential catalysis by the cholesterol side chain cleavage enzyme CYP11A1. *J. Biol. Chem.* **286,** 5607–5613
9. Strushkevich, N., MacKenzie, F., Cherkesova, T., Grabovec, I., Usanov, S., and Park, H. W. (2011) Structural basis for pregnenolone biosynthesis by the mitochondrial monooxygenase system. *Proc. Natl. Acad. Sci. U.S.A.* **108,** 10139–10143
10. Strushkevich, N., Gilep, A. A., Shen, L., Arrowsmith, C. H., Edwards, A. M., Usanov, S. A., and Park, H. W. (2013) Structural insights into aldosterone synthase substrate specificity and targeted inhibition. *Mol. Endocrinol.* **27,** 315–324
11. Annalora, A. J., Goodin, D. B., Hong, W. X., Zhang, Q., Johnson, E. F., and Stout, C. D. (2010) Crystal structure of CYP24A1, a mitochondrial cytochrome P450 involved in vitamin D metabolism. *J. Mol. Biol.* **396,** 441–451
12. Katagiri, M., Takikawa, O., Sato, H., and Suhara, K. (1977) Formation of a cytochrome P-450$_{scc}$-adrenodoxin complex. *Biochem. Biophys. Res. Commun.* **77,** 804–809
13. Seybert, D. W., Lambeth, J. D., and Kamin, H. (1978) The participation of a second molecule of adrenodoxin in cytochrome P-450-catalyzed 11β-hydroxylation. *J. Biol. Chem.* **253,** 8355–8358
14. Lambeth, J. D., and Kriengsiri, S. (1985) Cytochrome P-450$_{scc}$-adrenodoxin interactions: ionic effects on binding, and regulation of cytochrome reduction by bound steroid substrates. *J. Biol. Chem.* **260,** 8810–8816
15. Lambeth, J. D., Seybert, D. W., and Kamin, H. (1979) Ionic effects on adrenal steroidogenic electron transport: the role of adrenodoxin as an electron shuttle. *J. Biol. Chem.* **254,** 7255–7264
16. Lambeth, J. D., Seybert, D. W., and Kamin, H. (1980) Adrenodoxin reductase–adrenodoxin complex: rapid formation and breakdown of the complex and a slow conformational change in the flavoprotein. *J. Biol. Chem.* **255,** 4667–4672
17. Tuckey, R. C., and Kamin, H. (1982) The oxyferro complex of adrenal cytochrome P-450$_{scc}$: effect of cholesterol and intermediates on its stability and optical characteristics. *J. Biol. Chem.* **257,** 9309–9314
18. Hume, R., Kelly, R. W., Taylor, P. L., and Boyd, G. S. (1984) The catalytic cycle of cytochrome P-450$_{scc}$ and intermediates in the conversion of cholesterol to pregnenolone. *Eur. J. Biochem.* **140,** 583–591
19. Tuckey, R. C., Woods, S. T., and Tajbakhsh, M. (1997) Electron transfer to cytochrome P-450$_{scc}$ limits cholesterol-side-chain-cleavage activity in the human placenta. *Eur. J. Biochem.* **244,** 835–839
20. Beckert, V., and Bernhardt, R. (1997) Specific aspects of electron transfer from adrenodoxin to cytochromes P450$_{scc}$ and P45011β. *J. Biol. Chem.* **272,** 4883–4888
21. Schiffler, B., Zöllner, A., and Bernhardt, R. (2004) Stripping down the mitochondrial cholesterol hydroxylase system, a kinetics study. *J. Biol. Chem.* **279,** 34269–34276
22. Guengerich, F. P., and Cheng, Q. (2011) Orphans in the human cytochrome P450 superfamily: approaches to discovering functions and relevance in pharmacology. *Pharmacol. Rev.* **63,** 684–699
23. Wu, Z. L., Bartleson, C. J., Ham, A. J., and Guengerich, F. P. (2006) Heterologous expression, purification, and properties of human cytochrome P450 27C1. *Arch. Biochem. Biophys.* **445,** 138–146
24. Enright, J. M., Toomey, M. B., Sato, S. Y., Temple, S. E., Allen, J. R., Fujiwara, R., Kramlinger, V. M., Nagy, L. D., Johnson, K. M., Xiao, Y., How, M. J., Johnson, S. L., Roberts, N. W., Kefalov, V. J., Guengerich, F. P., and Corbo, J. C. (2015) Cyp27c1 red-shifts the spectral sensitivity of photoreceptors by converting vitamin A_1 into A_2. *Curr. Biol.* **25,** 3048–3057
25. Kramlinger, V. M., Nagy, L. D., Fujiwara, R., Johnson, K. M., Phan, T. T., Xiao, Y., Enright, J. M., Toomey, M. B., Corbo, J. C., and Guengerich, F. P. (2016) Human cytochrome P450 27C1 catalyzes 3,4-desaturation of retinoids. *FEBS Lett.* **590,** 1304–1312
26. Cho, H. P., Nakamura, M., and Clarke, S. D. (1999) Cloning, expression, and fatty acid regulation of the human Δ-5 desaturase. *J. Biol. Chem.* **274,** 37335–37339
27. Cooper, H. L., Mishra, G., Huang, X., Pender-Cudlip, M., Austin, R. N., Shanklin, J., and Groves, J. T. (2012) Parallel and competitive pathways for substrate desaturation, hydroxylation, and radical rearrangement by the non-heme diiron hydroxylase AlkB. *J. Am. Chem. Soc.* **134,** 20365–20375
28. Morikawa, T., Mizutani, M., Aoki, N., Watanabe, B., Saga, H., Saito, S., Oikawa, A., Suzuki, H., Sakurai, N., Shibata, D., Wadano, A., Sakata, K., and Ohta, D. (2006) Cytochrome P450 CYP710A encodes the sterol C-22 desaturase in *Arabidopsis* and tomato. *Plant Cell* **18,** 1008–1022
29. Arnqvist, L., Persson, M., Jonsson, L., Dutta, P. C., and Sitbon, F. (2008) Overexpression of CYP710A1 and CYP710A4 in transgenic *Arabidopsis* plants increases the level of stigmasterol at the expense of sitosterol. *Planta* **227,** 309–317
30. Skaggs, B. A., Alexander, J. F., Pierson, C. A., Schweitzer, K. S., Chun, K. T., Koegel, C., Barbuch, R., and Bard, M. (1996) Cloning and characterization of the *Saccharomyces cerevisiae* C-22 sterol desaturase gene, encoding a second cytochrome P-450 involved in ergosterol biosynthesis. *Gene* **169,** 105–109
31. Kelly, S. L., Lamb, D. C., Baldwin, B. C., Corran, A. J., and Kelly, D. E. (1997) Characterization of *Saccharomyces cerevisiae* CYP61, sterol Δ^{22}-desaturase, and inhibition by azole antifungal agents. *J. Biol. Chem.* **272,** 9986–9988
32. Rettie, A. E., Rettenmeier, A. W., Howald, W. N., and Baillie, T. A. (1987) Cytochrome P-450 catalyzed formation of δ^4-VPA, a toxic metabolite of valproic acid. *Science* **235,** 890–893
33. Rettie, A. E., Boberg, M., Rettenmeier, A. W., and Baillie, T. A. (1988) Cytochrome P-450-catalyzed desaturation of valproic acid *in vitro*. *J. Biol. Chem.* **263,** 13733–13738
34. Guan, X., Fisher, M. B., Lang, D. H., Zheng, Y. M., Koop, D. R., and Rettie, A. E. (1998) Cytochrome P450-dependent desaturation of lauric acid: isoform selectivity and mechanism of formation of 11-dodecenoic acid. *Chem.-Biol. Interact.* **110,** 103–121

35. Guengerich, F. P. (2001) Common and uncommon cytochrome P450 reactions related to metabolism and chemical toxicity. *Chem. Res. Toxicol.* **14,** 611–650
36. Wang, R. W., Kari, P. H., Lu, A. Y., Thomas, P. E., Guengerich, F. P., and Vyas, K. P. (1991) Biotransformation of lovastatin. IV. Identification of cytochrome P450 3A proteins as the major enzymes responsible for the oxidative metabolism of lovastatin in rat and human liver microsomes. *Arch. Biochem. Biophys.* **290,** 355–361
37. Kumar, D., De Visser, S. P., and Shaik, S. (2004) Oxygen economy of cytochrome P450: what is the origin of the mixed functionality as a dehydrogenase-oxidase enzyme compared with its normal function? *J. Am. Chem. Soc.* **126,** 5072–5073
38. Ji, L., Faponle, A. S., Quesne, M. G., Sainna, M. A., Zhang, J., Franke, A., Kumar, D., van Eldik, R., Liu, W., and de Visser, S. P. (2015) Drug metabolism by cytochrome P450 enzymes: what distinguishes the pathways leading to substrate hydroxylation over desaturation? *Chemistry* **21,** 9083–9092
39. Whitehouse, C. J., Bell, S. G., and Wong, L. L. (2008) Desaturation of alkylbenzenes by cytochrome P450(BM3) (CYP102A1). *Chemistry* **14,** 10905–10908
40. Bell, S. G., Zhou, R., Yang, W., Tan, A. B., Gentleman, A. S., Wong, L. L., and Zhou, W. (2012) Investigation of the substrate range of CYP199A4: modification of the partition between hydroxylation and desaturation activities by substrate and protein engineering. *Chemistry* **18,** 16677–16688
41. Törmä, H., and Vahlquist, A. (1985) Biosynthesis of 3-dehydroretinol (vitamin A_2) from all-*trans*-retinol (vitamin A_1) in human epidermis. *J. Invest. Dermatol.* **85,** 498–500
42. Daniels, F., and Alberty, R. A. (1966) *Physical Chemistry*, 3rd Ed., pp. 330–331, Wiley, New York
43. Johnson, K. A. (2003) Introduction to kinetic analysis of enzyme systems. In *Kinetic Analysis of Macromolecules: A Practical Approach* (Johnson, K. A., ed) pp. 1–18, Oxford University Press, Oxford, UK
44. Pallan, P. S., Nagy, L. D., Lei, L., Gonzalez, E., Kramlinger, V. M., Azumaya, C. M., Wawrzak, Z., Waterman, M. R., Guengerich, F. P., and Egli, M. (2015) Structural and kinetic basis of steroid 17α,20-lyase activity in teleost fish cytochrome P450 17A1 and its absence in cytochrome P450 17A2. *J. Biol. Chem.* **290,** 3248–3268
45. Lambeth, J. D., and Kamin, H. (1977) Adrenodoxin reductase and adrenodoxin: Mechanisms of reduction of ferricyanide and cytochrome *c*. *J. Biol. Chem.* **252,** 2908–2917
46. Guengerich, F. P., Krauser, J. A., and Johnson, W. W. (2004) Rate-limiting steps in oxidations catalyzed by rabbit cytochrome P450 1A2. *Biochemistry* **43,** 10775–10788
47. Guengerich, F. P. (2013) Kinetic deuterium isotope effects in cytochrome P450 oxidation reactions. *J. Labelled Comp. Radiopharm.* **56,** 428–431
48. Popa, C., Dicker, A. J., Dahler, A. L., and Saunders, N. A. (1999) Cytochrome P450, CYP26AI, is expressed at low levels in human epidermal keratinocytes and is not retinoic acid-inducible. *Br. J. Dermatol.* **141,** 460–468
49. Janmohamed, A., Dolphin, C. T., Phillips, I. R., and Shephard, E. A. (2001) Quantification and cellular localization of expression in human skin of genes encoding flavin-containing monooxygenases and cytochromes P450. *Biochem. Pharmacol.* **62,** 777–786
50. Yengi, L. G., Xiang, Q., Pan, J., Scatina, J., Kao, J., Ball, S. E., Fruncillo, R., Ferron, G., and Roland Wolf, C. (2003) Quantitation of cytochrome P450 mRNA levels in human skin. *Anal. Biochem.* **316,** 103–110
51. Du, L., Hoffman, S. M., and Keeney, D. S. (2004) Epidermal CYP2 family cytochromes P450. *Toxicol. Appl. Pharmacol.* **195,** 278–287
52. Swanson, H. I. (2004) Cytochrome P450 expression in human keratinocytes: an aryl hydrocarbon receptor perspective. *Chem.-Biol. Interact.* **149,** 69–79
53. Oesch, F., Fabian, E., Oesch-Bartlomowicz, B., Werner, C., and Landsiedel, R. (2007) Drug-metabolizing enzymes in the skin of man, rat, and pig. *Drug Metab. Rev.* **39,** 659–698
54. Ohno, Y., Nakamichi, S., Ohkuni, A., Kamiyama, N., Naoe, A., Tsujimura, H., Yokose, U., Sugiura, K., Ishikawa, J., Akiyama, M., and Kihara, A. (2015) Essential role of the cytochrome P450 CYP4F22 in the production of acylceramide, the key lipid for skin permeability barrier formation. *Proc. Natl. Acad. Sci. U.S.A.* **112,** 7707–7712
55. Andersson, E., Björklind, C., Törmä, H., and Vahlquist, A. (1994) The metabolism of vitamin A to 3,4-didehydroretinol can be demonstrated in human keratinocytes, melanoma cells and HeLa cells, and is correlated to cellular retinoid-binding protein expression. *Biochim. Biophys. Acta* **1224,** 349–354
56. Gygi, S. P., Rochon, Y., Franza, B. R., and Aebersold, R. (1999) Correlation between protein and mRNA abundance in yeast. *Mol. Cell. Biol.* **19,** 1720–1730
57. Uhlén, M., Fagerberg, L., Hallström, B. M., Lindskog, C., Oksvold, P., Mardinoglu, A., Sivertsson, Å., Kampf, C., Sjöstedt, E., Asplund, A., Olsson, I., Edlund, K., Lundberg, E., Navani, S., Szigyarto, C. A., *et al.* (2015) Tissue-based map of the human proteome. *Science* **347,** 1260419
58. Törmä, H., Asselineau, D., Andersson, E., Martin, B., Reiniche, P., Chambon, P., Shroot, B., Darmon, M., and Vahlquist, A. (1994) Biologic activities of retinoic acid and 3,4-didehydroretinoic acid in human keratinocytes are similar and correlate with receptor affinities and transactivation properties. *J. Invest. Dermatol.* **102,** 49–54
59. Vahlquist, A., Lee, J. B., Michaëlsson, G., and Rollman, O. (1982) Vitamin A in human skin. II. Concentrations of carotene, retinol and dehydroretinol in various components of normal skin. *J. Invest. Dermatol.* **79,** 94–97
60. Vahlquist, A. (1980) The identification of dehydroretinol (vitamin A_2) in human skin. *Experientia* **36,** 317–318
61. Vahlquist, A., Andersson, E., Coble, B. I., Rollman, O., and Törmä, H. (1996) Increased concentrations of 3,4-didehydroretinol and retinoic acid-binding protein (CRABPII) in human squamous cell carcinoma and keratoacanthoma but not in basal cell carcinoma of the skin. *J. Invest. Dermatol.* **106,** 1070–1074
62. Tafrova, J. I., Pinkas-Sarafova, A., Stolarzewicz, E., Parker, K. A., and Simon, M. (2012) UVA/B exposure promotes the biosynthesis of dehydroretinol in cultured human keratinocytes. *Mol. Cell. Biochem.* **364,** 351–361
63. Distlerath, L. M., and Guengerich, F. P. (1987) Enzymology of human liver cytochromes P-450, in *Mammalian Cytochromes P-450*, Vol. 1 (Guengerich, F. P., ed) pp. 133–198, CRC Press, Inc., Boca Raton, FL
64. Fukasawa, Y., Tsuji, J., Fu, S. C., Tomii, K., Horton, P., and Imai, K. (2015) MitoFates: improved prediction of mitochondrial targeting sequences and their cleavage sites. *Mol. Cell. Proteomics* **14,** 1113–1126
65. Ortiz de Montellano, P. R. (2015) Substrate oxidation, in *Cytochrome P450: Structure, Mechanism, and Biochemistry*, 4th Ed. (Ortiz de Montellano, P. R., ed) pp. 111–176, Springer, New York
66. Guengerich, F. P., and Kim, D.-H. (1991) Enzymatic oxidation of ethyl carbamate to vinyl carbamate and its role as an intermediate in the formation of 1,N^6-ethenoadenosine. *Chem. Res. Toxicol.* **4,** 413–421
67. Fersht, A. (1999) *Structure and Mechanism in Protein Science*, pp. 158–159, Freeman, New York
68. Yun, C. H., Kim, K. H., Calcutt, M. W., and Guengerich, F. P. (2005) Kinetic analysis of oxidation of coumarins by human cytochrome P450 2A6. *J. Biol. Chem.* **280,** 12279–12291
69. Isin, E. M., and Guengerich, F. P. (2006) Kinetics and thermodynamics of ligand binding by cytochrome P450 3A4. *J. Biol. Chem.* **281,** 9127–9136
70. Pallan, P. S., Wang, C., Lei, L., Yoshimoto, F. K., Auchus, R. J., Waterman, M. R., Guengerich, F. P., and Egli, M. (2015) Human cytochrome P450 21A2, the major steroid 21-hydroxylase: structure of the enzyme-progesterone substrate complex and rate-limiting C–H bond cleavage. *J. Biol. Chem.* **290,** 13128–13143
71. Griffin, B. W., and Peterson, J. A. (1972) Camphor binding by *Pseudomonas putida* cytochrome P-450: kinetics and thermodynamics of the reaction. *Biochemistry* **11,** 4740–4746
72. Sevrioukova, I. F., and Poulos, T. L. (2012) Structural and mechanistic insights into the interaction of cytochrome P450 3A4 with bromoergocryptine, a Type I ligand. *J. Biol. Chem.* **287,** 3510–3517
73. Guengerich, F. P., and Johnson, W. W. (1997) Kinetics of ferric cytochrome P450 reduction by NADPH-cytochrome P450 reductase: rapid reduction in the absence of substrate and variations among cytochrome P450 systems. *Biochemistry* **36,** 14741–14750

74. Stevens, V. L., Aw, T. Y., Jones, D. P., and Lambeth, J. D. (1984) Oxygen dependence of adrenal cortex cholesterol side chain cleavage: implications in the rate-limiting steps in steroidogenesis. *J. Biol. Chem.* **259,** 1174–1179
75. Fasco, M. J., Dymerski, P. P., Wos, J. D., and Kaminsky, L. S. (1978) A new warfarin metabolite: structure and function. *J. Med. Chem.* **21,** 1054–1059
76. Nagata, K., Liberato, D. J., Gillette, J. R., and Sasame, H. A. (1986) An unusual metabolite of testosterone: 17β-4,6-androstadiene-3-one. *Drug Metab. Dispos.* **14,** 559–565
77. Broun, P., Shanklin, J., Whittle, E., and Somerville, C. (1998) Catalytic plasticity of fatty acid modification enzymes underlying chemical diversity of plant lipids. *Science* **282,** 1315–1317
78. Broadwater, J. A., Whittle, E., and Shanklin, J. (2002) Desaturation and hydroxylation: residues 148 and 324 of *Arabidopsis* FAD2, in addition to substrate chain length, exert a major influence in partitioning of catalytic specificity. *J. Biol. Chem.* **277,** 15613–15620
79. Wang, B., Lee, Y.-M., Clémancey, M., Seo, M. S., Sarangi, R., Latour, J.-M., and Nam, W. (2016) Mononuclear nonheme high-spin iron(III)-acylperoxo complexes in olefin epoxidation and alkane hydroxylation reactions. *J. Am. Chem. Soc.* **138,** 2426–2436
80. Rishavy, M. A., Hallgren, K. W., Wilson, L. A., Usubalieva, A., Runge, K. W., and Berkner, K. L. (2013) The vitamin K oxidoreductase is a multimer that efficiently reduces vitamin K epoxide to hydroquinone to allow vitamin K-dependent protein carboxylation. *J. Biol. Chem.* **288,** 31556–31566
81. Massey, V., and Hemmerich, P. (1977) A photochemical procedure for reduction of oxidation-reduction proteins employing deazariboflavin as catalyst. *J. Biol. Chem.* **252,** 5612–5614
82. Yoshimoto, F. K., Jung, I. J., Goyal, S., Gonzalez, E., and Guengerich, F. P. (2016) Isotope-labeling studies support the electrophilic Compound I iron active species, FeO^{3+}, for the carbon-carbon bond cleavage reaction of the cholesterol side-chain cleavage enzyme, cytochrome P450 11A1. *J. Am. Chem. Soc.* **138,** 12124–12141
83. Ačimovič, J., Goyal, S., Košir, R., Goličnik, M., Perše, M., Belič, A., Urlep, Ž., Guengerich, F. P., and Rozman, D. (2016) Cytochrome P450 metabolism of the post-lanosterol intermediates explains enigmas of cholesterol synthesis. *Sci. Rep.* **6,** 28462
84. Thomas, P. E., Korzeniowski, D., Ryan, D., and Levin, W. (1979) Preparation of monospecific antibodies against two forms of rat liver cytochrome P-450 and quantitation of these antigens in microsomes. *Arch. Biochem. Biophys.* **192,** 524–532
85. Guengerich, F. P., Wang, P., and Davidson, N. K. (1982) Estimation of isozymes of microsomal cytochrome P-450 in rats, rabbits, and humans using immunochemical staining coupled with sodium dodecyl sulfate-polyacrylamide gel electrophoresis. *Biochemistry* **21,** 1698–1706
86. Shevchenko, A., Tomas, H., Havlis, J., Olsen, J. V., and Mann, M. (2006) In-gel digestion for mass spectrometric characterization of proteins and proteomes. *Nat. Prot.* **1,** 2856–2860
87. MacLean, B., Tomazela, D. M., Shulman, N., Chambers, M., Finney, G. L., Frewen, B., Kern, R., Tabb, D. L., Liebler, D. C., and MacCoss, M. J. (2010) Skyline: an open source document editor for creating and analyzing targeted proteomics experiments. *Bioinformatics* **26,** 966–968
88. Tabb, D. L., Fernando, C. G., and Chambers, M. C. (2007) MyriMatch: highly accurate tandem mass spectral peptide identification by multivariate hypergeometric analysis. *J. Proteome Res.* **6,** 654–661
89. Holman, J. D., Ma, Z. Q., and Tabb, D. L. (2012) Identifying proteomic LC-MS/MS data sets with Bumbershoot and IDPicker. *Curr. Protocol. Bioinformatics* 10.1002/0471250953.bi1317s37
90. Foust, G. P., Burleigh, B. D., Jr., Mayhew, S. G., Williams, C. H., Jr., and Massey, V. (1969) An anaerobic titration assembly for spectrophotometric use. *Anal. Biochem.* **27,** 530–535
91. Burleigh, B. D., Jr., Foust, G. P., and Williams, C. H., Jr. (1969) A method for titrating oxygen-sensitive organic redox systems with reducing agents in solution. *Anal. Biochem.* **27,** 536–544
92. Patil, P. V., and Ballou, D. P. (2000) The use of protocatechuate dioxygenase for maintaining anaerobic conditions in biochemical experiments. *Anal. Biochem.* **286,** 187–192
93. Palfey, B. A. (2003) Time resolved spectral analysis. In *Kinetic Analysis of Macromolecules* (Johnson, K. A., ed) pp. 203–228, Oxford University Press, New York
94. Guengerich, F. P. (2014) Analysis and characterization of enzymes and nucleic acids relevant to toxicology. In *Hayes' Principles and Methods of Toxicology* (Hayes, A. W., and Kruger, C. L., eds) pp. 1905–1964, 6th Ed., CRC Press-Taylor & Francis, Boca Raton, FL
95. Nelson, D. R. (2009) The cytochrome P450 homepage. *Hum. Genomics* **4,** 59–65